



## Bridgewater State University Virtual Commons - Bridgewater State University

Honors Program Theses and Projects

Undergraduate Honors Program

5-9-2017

# Geochemical and Petrographic Analysis of Basaltic Rocks of the Hawaiian Island: Implications for their Evolutionary Stage of Development

Autumn A. Burrell

Follow this and additional works at: [http://vc.bridgew.edu/honors\\_proj](http://vc.bridgew.edu/honors_proj)



Part of the [Geochemistry Commons](#)

### Recommended Citation

Burrell, Autumn A.. (2017). Geochemical and Petrographic Analysis of Basaltic Rocks of the Hawaiian Island: Implications for their Evolutionary Stage of Development. In *BSU Honors Program Theses and Projects*. Item 205. Available at: [http://vc.bridgew.edu/honors\\_proj/205](http://vc.bridgew.edu/honors_proj/205)  
Copyright © 2017 Autumn A. Burrell

This item is available as part of Virtual Commons, the open-access institutional repository of Bridgewater State University, Bridgewater, Massachusetts.

Geochemical and Petrographic Analysis of Basaltic Rocks of the Hawaiian Island: Implications for their  
Evolutionary Stage of Development

Autumn A. Burrell

Submitted in Partial Completion of the  
Requirements for Commonwealth Honors in Geological Sciences

Bridgewater State University

May 9, 2017

Dr. Michael A. Krol, Thesis Director  
Dr. Christine M. Brandon, Committee Member  
Dr. Richard L. Enright, Committee Member

## TABLE OF CONTENTS

## PAGE #

LIST OF FIGURES.....	2
ACKNOWLEDGEMENTS.....	4
ABSTRACT.....	5
INTRODUCTION .....	6
GEOLOGIC SETTING.....	10
METHODOLOGY.....	13
RESULTS.....	21
DISCUSSION.....	42
REFERENCES CITED.....	50

<b>LIST OF FIGURES</b>	<b>PAGE #</b>
1.) Bowen's Reaction Series, which shows the fractional crystallization sequence of different minerals...	8
2.) A schematic cross section of a typical shield volcano.....	8
3.) The evolutionary stages of volcanoes.....	12
4.) Map of the five different volcanoes on the Big Island of Hawaii.....	12
5.) Depiction of Hawaiian Volcano ages and their relation to their distance from Kilauea.....	13
6.) Location map of rock samples collected across the Big Island of Hawaii with legend.....	14
7.) This photograph shows the Braun Chipmunk Rock Crusher.....	17
8.) This photograph shows the SPEX mixer ball mill 8000.....	18
9.) This photograph shows the Rocklabs Bench Top Ring Mill (BTRM).....	18
10.) This photograph shows a disk mill that was used to achieve sand-sized samples.....	19
11.) This photograph shows a 25-ton press used to make pressed pellets.....	19
12.) This photograph shows a muffle furnace where samples were melted at 1000 ° C in graphite crucible	20
13.) This photograph shows pressed pellets and fusion beads undergoing geochemical analysis in the Rigaku ZSX-3 XRF machine.....	20
14.) A rock sample, showing the variety in texture and crystal size (~ 3 cm) of olivine.....	24
15.) Photomicrograph from KO-1.....	24
16.) Photomicrograph from KO-2.....	25
17.) Photomicrograph from HU-1.....	25
18.) Photomicrograph from MK-1.....	26
19.) Photomicrograph from MK-3.....	26
20.) Photomicrograph from ML-4.....	27
21.) Photomicrograph from KI-6.....	27
22.) CaO vs. SiO <sub>2</sub> graph from Kohala volcanics. ....	30
23.) CaO vs. MgO graph from Kohala volcanics. ....	30
24.) Al <sub>2</sub> O <sub>3</sub> vs. SiO <sub>2</sub> graph from Kohala volcanics. ....	31
25.) Al <sub>2</sub> O <sub>3</sub> vs. MgO graph from Kohala volcanics. ....	31
26.) TiO <sub>2</sub> vs. SiO <sub>2</sub> graph from Kohala volcanics. ....	32

27.) $\text{Al}_2\text{O}_3$ vs. MgO graph from Hualalai volcanics.....	32
28.) $\text{Al}_2\text{O}_3$ vs. $\text{SiO}_2$ graph from Hualalai volcanics.....	33
29.) CaO vs. MgO graph from Hualalai volcanics.....	33
30.) CaO vs. $\text{SiO}_2$ graph from Hualalai volcanics.....	34
31.) $\text{TiO}_2$ vs. $\text{SiO}_2$ graph from Hualalai volcanics. ....	34
32.) $\text{TiO}_2$ vs. $\text{SiO}_2$ graph from Mauna Kea volcanics. ....	35
33.) CaO vs. $\text{SiO}_2$ graph from Mauna Kea volcanics.....	35
34.) CaO vs. MgO graph from Mauna Kea volcanics.....	36
35.) $\text{Al}_2\text{O}_3$ vs. $\text{SiO}_2$ graph from Mauna Kea volcanics.....	36
36.) $\text{Al}_2\text{O}_3$ vs. MgO graph from Mauna Kea volcanics. ....	37
37.) $\text{Al}_2\text{O}_3$ vs. MgO graph from Mauna Loa volcanics. ....	37
38.) $\text{Al}_2\text{O}_3$ vs. $\text{SiO}_2$ graph from Mauna Loa volcanics.....	38
39.) CaO vs. MgO graph from Mauna Loa volcanics. ....	38
40.) CaO vs. $\text{SiO}_2$ graph from Mauna Loa volcanics. ....	39
41.) $\text{TiO}_2$ vs. $\text{SiO}_2$ graph from Mauna Loa volcanics. ....	39
42.) $\text{TiO}_2$ vs. $\text{SiO}_2$ graph from Kilauea volcanics.....	40
43.) CaO vs. $\text{SiO}_2$ graph from Kilauea volcanics.....	40
44.) CaO vs. MgO graph from Kilauea volcanics.....	41
45.) $\text{Al}_2\text{O}_3$ vs. $\text{SiO}_2$ graph from Kilauea volcanics.....	41
46.) $\text{Al}_2\text{O}_3$ vs. MgO graph from Kilauea volcanics.....	42
47.) Total alkali vs. $\text{SiO}_2$ graph depicting tholeiitic and alkalic fields based on their chemical composition...46	
48.) Tectonic discrimination diagram of Zr/Y vs. Zr showing the tectonic settings for basalt.....	47
49.) Tectonic discrimination diagram further defining tectonic settings of basalt generation.....	48
50.) Tectonic discrimination diagram further defining tectonic settings of basalt generation.....	49

## **ACKNOWLEDGEMENTS**

First and foremost, I would like to give a huge thank you to my advisor, Dr. Michael A. Krol. I am immensely grateful and feel blessed for your guidance throughout this process as well as your tremendous amount of patience and support. I greatly appreciate all of the time you have dedicated to this research project, and helping me grow as a geologist. I know that I could not have done this without you.

The Bridgewater State University Department of Geological Sciences as a whole has also been very supportive of my endeavors. I appreciate Dr. Enright for introducing us to a fascinating field site. I would also like to thank Dr. Enright and Dr. Brandon for their constructive criticism. Thank you to Jessica Campbell for her patience and guidance in teaching me all the different laboratory techniques needed to successfully complete this thesis.

Lastly, I would like to thank my family for their continued support throughout my life. Specifically, I would like to thank my dad for his positivity throughout my time at Bridgewater. There were many times I did not believe in myself, but you have always believed in me. I would like to thank my mom for telling me to “follow my heart”, in terms of picking a major. I’m glad I listened, or else I wouldn’t be where I am today. To my brother, you grew up so fast. Thank you for always having a great sense of humor and being one of the best people I know.

## **ABSTRACT**

Geochemical and petrographic analyses of basaltic rocks were performed from five volcanoes on the Big Island of Hawaii. From north to south these volcanoes include: Kohala; Hualalai; Mauna Kea; Mauna Loa; and Kilauea. These volcanoes have formed through several distinct stages of volcanic growth and development. During each of these stages, the lavas extruded will be composed of a distinctive geochemical signature which corresponds to each of the 4 main phases of development. These include a 1) pre-shield building; 2) main shield building; 3) post-shield building; and 4) a rejuvenated stage.

The geochemical results are used to establish the evolutionary stage each volcano is in and provide insight on the sources of the magma driving these eruptions. Over 50 samples were collected from a variety of prehistoric and historic lava flows on Hawaii and prepared in the Department of Geological Sciences. These samples were analyzed for major oxides and trace elements using X-ray fluorescence (XRF) techniques. In addition, a detailed petrographic analysis of thin sections was performed on each of the samples, allowing the mineralogy and textures of these lava flows to be identified. Petrographic results were combined with geochemical results to develop a model for the source of the magma and how it has changed over time. The goal of this project is to investigate the changes in geochemical signature with respect to time and position related to the mantle plume beneath the island of Hawaii and determine the eruptive stage of the volcano based on the geochemistry of the different basalts. The intent was to discover the current stage of development for each of the volcanoes.

## INTRODUCTION

Volcanoes can be associated with many different geological settings, such as mid-oceanic spreading centers, subduction zones, or intraplate hot spots. A hot spot is an area that has experienced magmatic activity commonly associated with large mantle plumes. Molten magma from the mantle plume feeds a volcanic center resulting in long-lived activity. The position of volcanoes over a hotspot can change location because the lithospheric plate does not remain stationary over the mantle plume. As their location changes, the geochemistry of the extruding lava can also change. In addition to location change, the mechanics of the depth of melting and the percentage of the mantle that is melting, can also affect the geochemistry. Therefore, the geochemistry of the older lava flows can provide information on the evolutionary stage of development for a particular volcano, and how it changes over time.

The chemical composition of the lava is thought to change for different reasons. One possible reason for this, is that the mantle melt below the island of Hawaii produces magma that contains a weight percent of approximately 17 of magnesium oxide (Clague and Denlinger, 1994). The rising of the magma, will cause minerals to crystallize at different times due to differential cooling. This idea is based on Bowen's Reaction Series (Figure 1). Crystals will crystallize at different temperatures. If the crystal is denser than the magma surrounding it, the crystal will begin to settle and as a result will be removed from the magma (Clague and Denlinger, 1994). This crystal removal from the magma, will cause the chemical composition to shift. For example, if olivine crystals gradually began to settle to the bottom of the magma chamber, the magma that is erupting will have progressively less and less magnesium oxide and have more silica (Clague and Denlinger, 1994). Over time many volcanoes ultimately tend to change from a picrite composition to a basaltic composition (Clague and Denlinger, 1994). A



basaltic rock is a fine-grained, mafic or magnesium-rich, igneous rock and can be vesicular and amygdaloidal in texture. (Jerram & Petford, 2011) A picrite is also an igneous rock that is mainly composed of olivine.

There are four main types of volcanoes, which include cinder cones, composite, lava domes, and shield volcanoes (Watson, 2001). The volcanic rocks collected for this research project are all basaltic rocks which were the products of shield volcanic eruptions. Shield volcanoes are characterized by gentle slopes and resemble the shape of a dome, which are formed from the outpouring of “thousands of highly fluid lava flows” from a “central summit vent” (Figure 2) (Watson 2001). Figure 2 shows the cross section of a typical shield volcano, which resembles the volcanoes on the Hawaiian island. These volcanoes have different stages of development. Figure 3 shows the formation and evolution of the volcanic islands associated with hotspot activity. There are three main stages of development. These include a pre-shield stage, a main shield building stage, and a post-shield stage which is included in the erosional stage. There is also a rejuvenation stage, which is characterized by alkalic lavas and the geochemistry indicates that the source is deep within the mantle (Chen & Frey, 1985). The pre-shield and post-shield stage is characterized by alkalic lavas, while the main building shield stage is characterized by tholeiitic lavas.

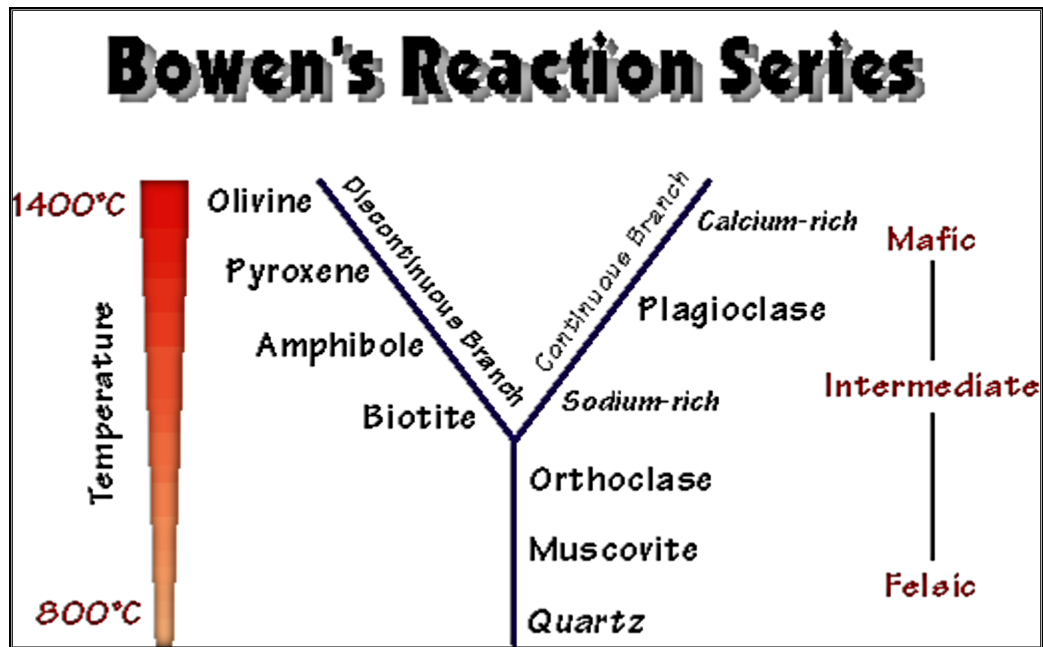


**Figure 1.** Bowen's Reaction Series, which shows the fractional crystallization sequence of different minerals (Strickler, 1997).

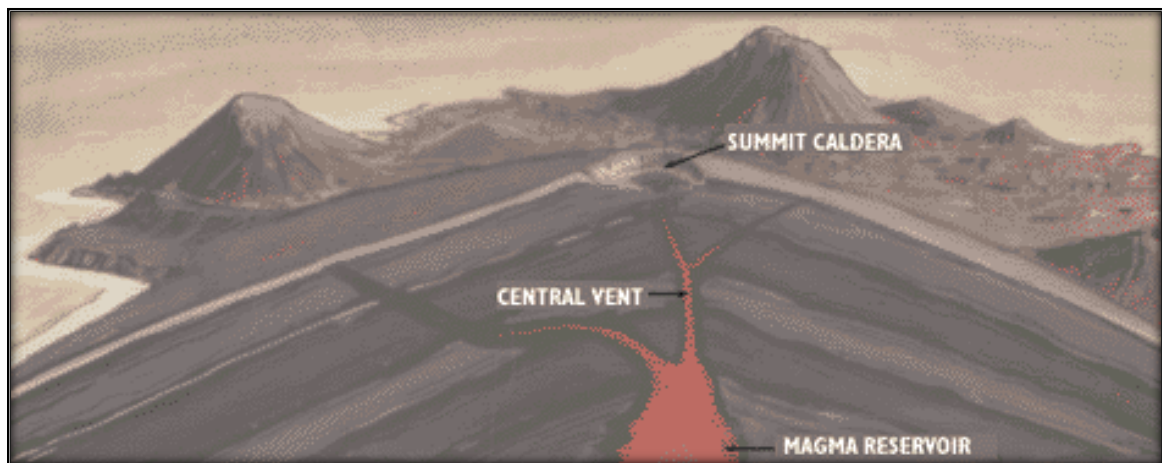


**Figure 2.** A schematic cross section of a typical shield volcano (Watson, 2001).

The geochemistry of lavas from the pre-shield and the post-shield stage typically display a more alkalic geochemical signature than those in the main shield building stage (Tardona, 2011). The geochemical signature of the lavas in the main shield building stage will be more tholeiitic in composition. This is due to the higher degree of partial melting within the main shield building stage. These volcanoes and enormous outpourings of lava are a result of the movement of the Pacific tectonic plate over a relatively stationary hot spot, or mantle plume. As the Pacific lithospheric plate moves, this will determine the composition of the magma that is provided to the volcanoes. This is because, depending on the location of the Pacific lithospheric plate with respect to the hotspot, the amount of partial melting and magma production will vary (Clague, 1987). “Small percentages of partial melting produce magma that is rich in alkali elements relative to silica, (called alkalic basalt)” (Clague, 1987). The reason for this is because sodium and potassium are generally incompatible elements that enter in a magma initially at the onset of melting.

The closer the volcano is to the hotspot, there is less silica content within the rock. This may indicate that it is in the pre-shield stage. As, the volcano moves away from the hotspot and its silica content increases, it transitions from the main shield stage to the post-shield stage. These lavas differ in age and chemistry, which is related to their position over a large mantle plume and the dynamics associated with melting that continually feeds magma to these volcanoes as the oceanic lithosphere moves over this hot spot and the source of magma feeding them. The geochemistry of these lavas changes over time and provides insight into the processes operating during their eruption activity. Therefore, based on the data collected concerning geochemical analysis of the Hawaiian basalts, the stages of each volcano may be determined using discrimination diagrams.

The purpose of this study is to evaluate the evolution of five volcanoes on the Big Island of Hawaii through their geochemical signatures and to determine their various stages of development. This will be done through the use of geochemical and petrographic analysis on rock samples from these volcanoes.

## **GEOLOGIC SETTING**

The Island of Hawaii, comprised of predominantly basaltic lava flows, is the result of hotspot activity within the Pacific lithospheric plate. A hotspot refers to a very large area (~500 to 600 km wide and up to ~2,000 km deep) that is undergoing melting and subsequent magmatic activity and volcanism resulting in production of new crust (Garcia, 2011). These hotspots are due to the existence of a large stationary mantle plume. The hot magma from the mantle plume rises through the colder oceanic crust of the Earth, resulting in volcanic activity concentrated above the plume.

In Hawaii, there are volcanoes exposed above the surface of the ocean, however some volcanoes never make it above the seafloor to the ocean surface. Because of the movement of the Pacific Plate over hundreds of thousands to millions of years, the volcanoes located here transition or evolve through several magmatic stages. As the plate motion continues away from the mantle plume, volcanic activity will gradually decline, and eventually cease. However, new volcanoes continue to form above the hotspot. They are a part of a long-lived hotspot track extending from Alaska to Hawaii, known as the Hawaiian island emperor seamount chain (Banks, 2015).

There are five different volcanoes on the Big Island of Hawaii, which are shown in figure 4. The age of the Hawaiian volcanoes, listed from youngest to oldest include: Kilauea, Mauna

Loa, Mauna Kea, Hualalai, Kohala (Garcia, 2011). The age of the volcanoes is believed to have a relation to the way the islands are constructed on the moving sea floor of the North Pacific Ocean (Garcia, 2011). “This movement takes it to the northwest compared to the layers below it at a rate of 5 to 10 cm/yr” (Garcia, 2011). The smaller the distance from Kilauea, the younger the volcano is in age (Figure 5).

Kilauea and Mauna Loa are currently in the main shield eruptive stage, whereas Hualalai, Mauna Kea, and Kohala are transitioning to the post-shield stage. In the main shield stage, volcanoes are characterized by high eruption rates and volumes, but in the post-shield stage, the eruption rates and volumes will diminish.

The rocks gathered from different flows, ranged in age from forming from 350, 000 years ago to closer in age to the present. The Kohala volcanic rocks range from 350, 000 to 150, 000 years old. The Mauna Kea volcanic rocks range from 150, 000 to 10, 000 years old. Hualalai volcanic rocks are predominantly less than 11, 000 years old, whereas the Mauna Loa volcanics are mainly from the 19<sup>th</sup> century. The Kilauea volcanics range in age from the 1960s to the present. All of the volcanic rocks were basaltic, some vesicular or aphanitic in texture, characterized by both pahoehoe and aa lava flows, and some containing olivine and plagioclase phenocrysts.

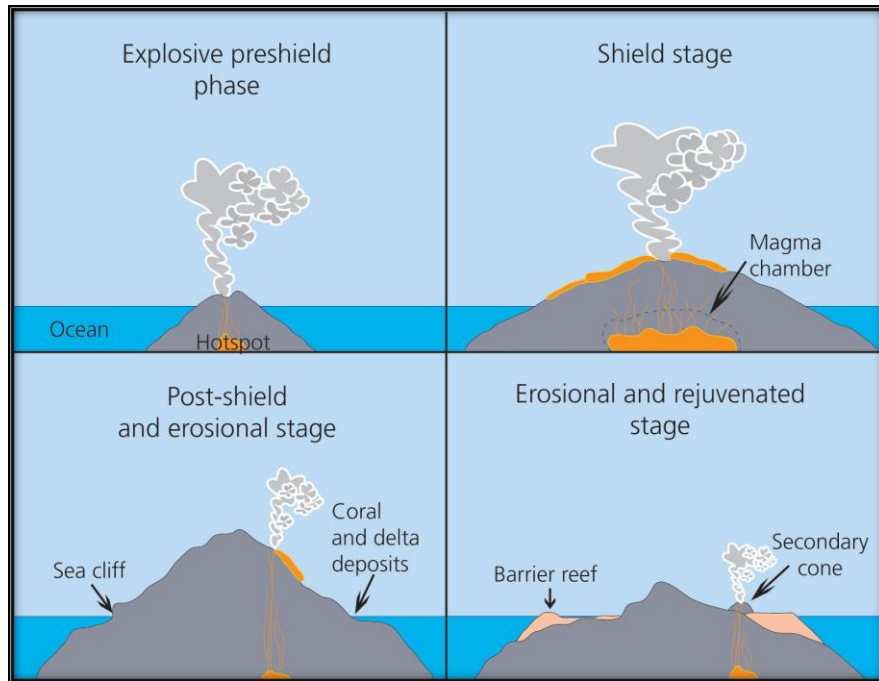


**Figure 3.** The evolutionary stages of volcanoes (Thornberry-Ehrlich, 2017).

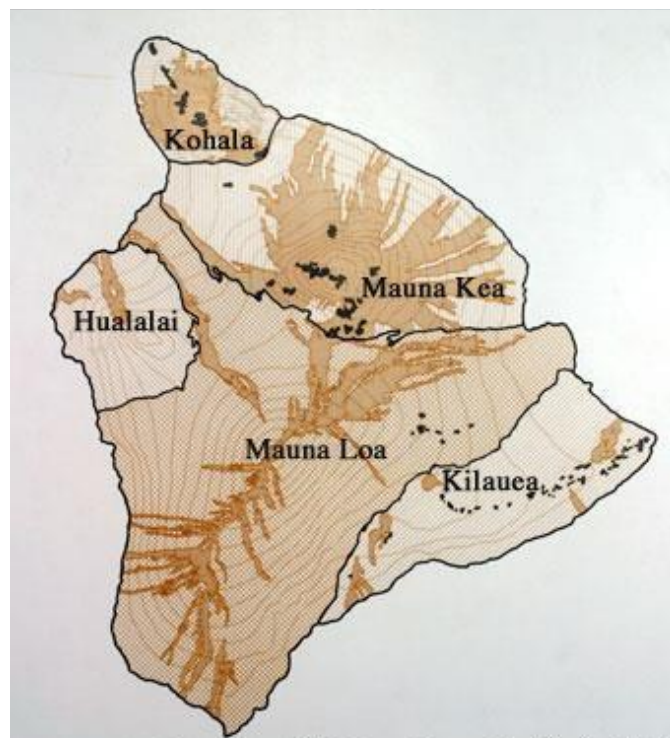


**Figure 4.** Map of the five different volcanoes on the Big Island of Hawaii (USGS Jaggar Museum 2008).

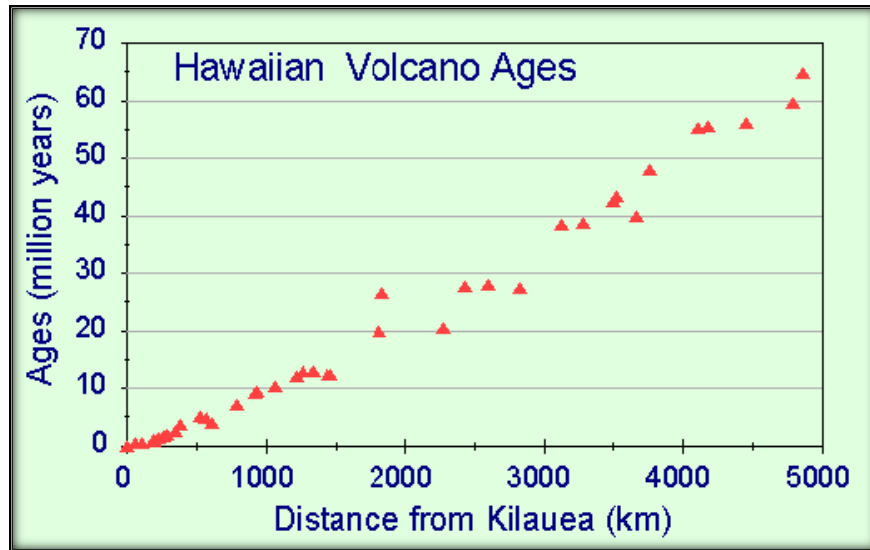


**Figure 5.** Depiction of Hawaiian Volcano ages and their relation to their distance from Kilauea. (Garcia, 2011)

## METHODOLOGY

### Fieldwork/Sample Collection

During a field trip in March 2016, rock samples were collected from five volcanoes on the Big Island of Hawaii. Fresh samples were collected from lava flows in an effort to evaluate the geochemistry of these volcanoes and how that chemistry has changed through time.

Wherever possible, fresh, unaltered basaltic rocks were sampled in order to ensure the representative geochemistry of these lavas. Samples were approximately fist-sized (8-12 cm) and taken from lava flows associated with the Kohala, Hualalai, Mauna Kea, Mauna Loa, and Kilauea volcanoes. Figure 6 shows the locations of samples collected in relation to the five shield volcanoes. Samples were shipped back to the Bridgewater State University Geology Department, where they were then further processed for petrographic and geochemical analyses.

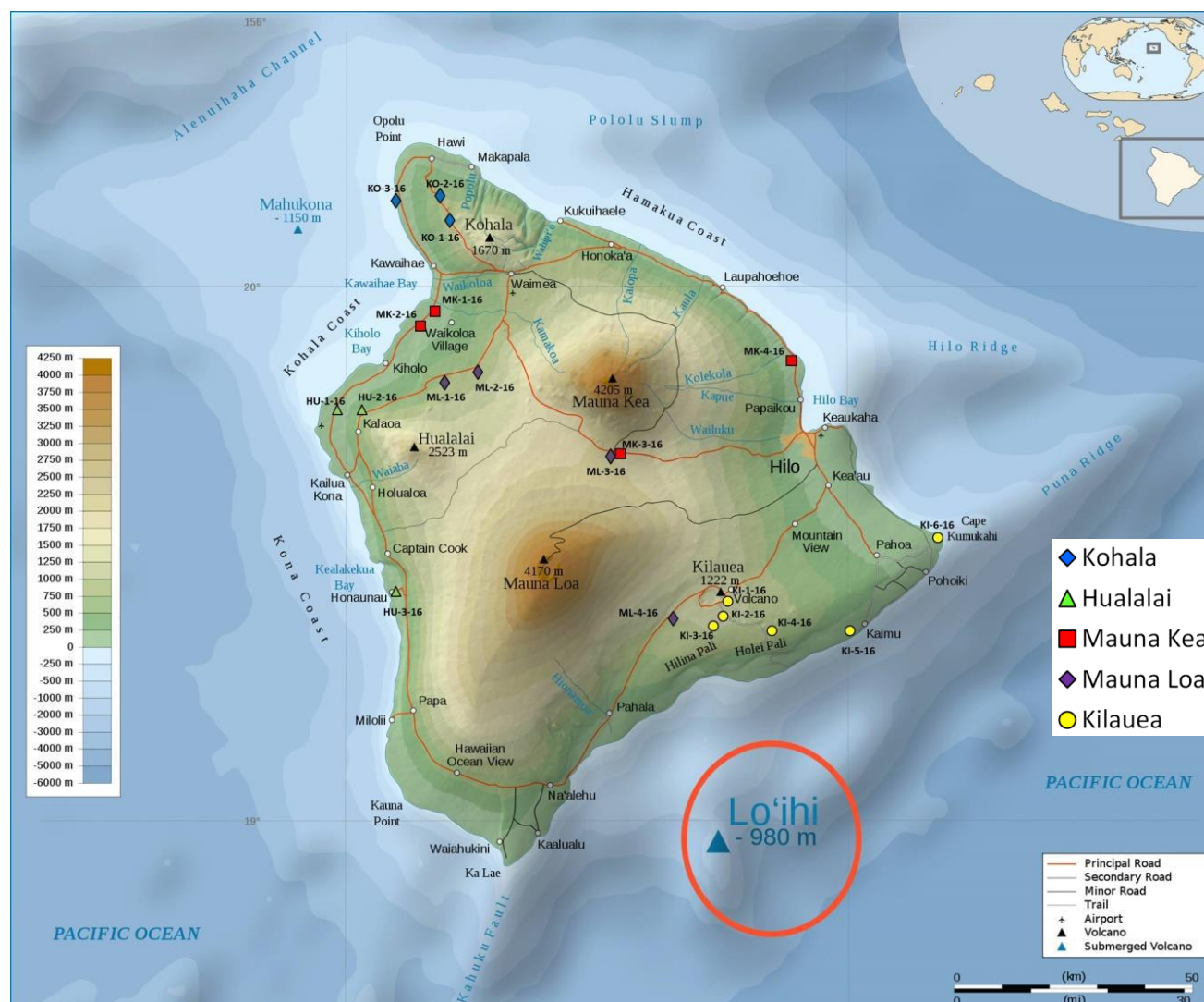


**Figure 6.** Location map of rock samples collected across the Big Island of Hawaii with legend.

## Sample Preparation for Geochemical Analysis

The rock samples were approximately 8-12 cm in diameter, and were broken into smaller pieces with a hammer. A jaw crusher then pulverized the rock into gravel-sized pieces (2-4 cm) (Figure 7). Approximately 20 g of the gravel-sized material was placed inside a ball mill and run for a duration of 30 minutes to an hour, and milled into a fine powder similar in grain size to talcum powder. Three mill machines were used in this process; the SPEX mixer mill 8000 (Figure 8), the Rocklabs Bench Top Ring Mill (BTRM) (Figure 9) and a disk mill (Figure 10).



During the milling process, the ball mill was stopped at every 5-10 minute intervals, so the sample vessel did not overheat. It was important to ensure each sample was ground to a consistent fine-grained powder prior to preparation for production as pressed pellets and fusion disks/beads for X-ray fluorescence analysis. The powdered sample was then prepared as pressed pellets and fusion beads to measure for trace elements and major oxides, respectively (Watanabe, 2015; Yamada, 2010).

### **Pressed Pellet Preparation to Analyze Trace Elements**

To prepare a pressed pellet, approximately 9.0 g of the powder sample was weighed and then dried for an hour to drive off any water present from the powder sample in a drying oven at ~100 °C. The sample was allowed to cool and re-weighed to determine the % H<sub>2</sub>O in the sample using the following equation:

$$\% H_2O = \left( \frac{\text{Weight prior to drying oven} - \text{Weight after drying oven}}{\text{Weight prior to drying oven}} \right) * 100$$

8.3000 ± 0.0003 g of the sample was placed in a mixing vial with 1.1312 ± 0.0003 g of SpectroBlend 44 μm Powder. Two mixing beads were added to a vial and the mixture was manually shaken for approximately 2-3 minutes to ensure complete mixing. The sample mixture was then transferred to a die set c-p and was compacted together, using a 25-ton tabletop press (Figure 11). Pressure was applied to the sample for a minute and thirty seconds at approximately 20 tons of pressure. A plunger was pressed through the die set until the pressed pellet was removed.

### **Fusion Bead Preparation to Analyze Major Oxides**

Prior to preparing a fusion bead, the loss on ignition (LOI) for each sample needed to be calculated. The loss on ignition accounts for any volatiles that may have been present in the sample. To do this, 0.2500 g of the sample powder was measured and placed into a graphite crucible. The crucible containing the sample was placed in a muffle furnace at 1020 °C for one hour (Figure 12), after which it was allowed to cool and reweighed.

These weights were used to calculate the loss on ignition using the following equation:

$$LOI = \frac{\text{Weight prior to the muffle furnace} - \text{Weight after the muffle furnace}}{\text{Weight prior to the muffle furnace}}$$

To prepare a fusion bead, ~2.00 g of the sample powder was dried out in a beaker identical to methods used for the pressed pellet preparation. Then, 1.2500 g  $\pm$  0.0003 g of the sample was mixed with 8.7500 g  $\pm$  0.0003 g of lithium borate. This was approximately a 1:7 ratio. This sample mixture, was then put in a graphite crucible, and heated in the muffle furnace for 20 minutes (Figure 12). At 5 minute intervals, the sample mixture was taken out, and manually swirled to promote the complete mixing of the material. Then, it was allowed to cool for an hour, and the result of the powder and lithium borate mixture was the formation of a fusion glass bead. The glass bead was then polished with micron polishing paper, prior to placing it into the XRF machine for analysis.

### **X-ray Fluorescence**

The samples were analyzed using x-ray fluorescence to determine the major oxides and trace elements present in the rocks (Figure 13). The instrument used for this technique was the

Rigaku ZSX Primus. The XRF system is fully automated and results were typically obtained within 24 hours. Using the data from the XRF, the geochemical data was analyzed to characterize the chemistry of the volcanic flows. The XRF instrument ran on a voltage of 3 kW. Both USGS, NIST, and Rigaku standards were used to calibrate the instrument.

### **Sample Preparation for Petrographic Analysis**

Each rock sample was cut and slabbed using a diamond embedded rock saw. Slabs were trimmed down to a ~0.5 cm thick chip, measuring 3 cm X 1.5 cm. Chips were sent to a commercial petrographic laboratory (Spectrum Petrographics, Inc.) where they were mounted to a glass slide and ground down to a final thickness of 30 microns. Each slide was covered with a cover slip.



**Figure 7.** This photograph shows the Braun Chipmunk Rock Crusher.

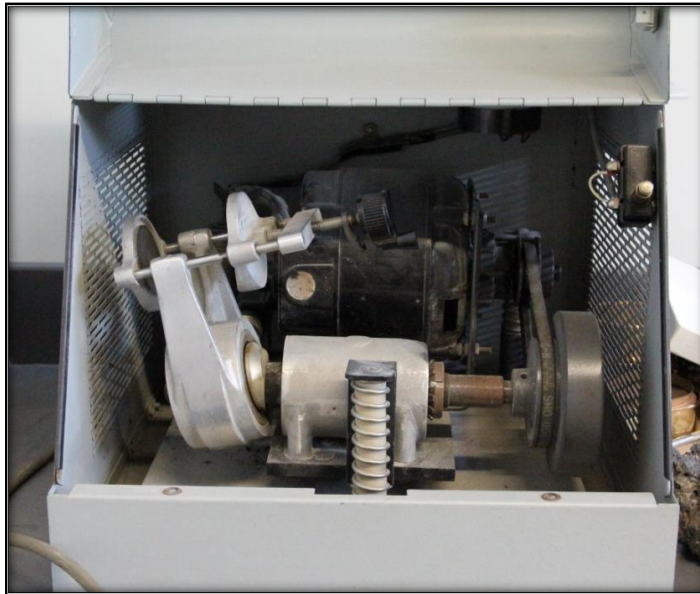


**Figure 8.** This photograph shows the SPEX mixer ball mill 8000.



**Figure 9.** This photograph shows the Rocklabs Bench Top Ring Mill (BTRM).



**Figure 10.** This photograph shows a disk mill that was used to achieve sand-sized samples.



**Figure 11.** This photograph shows a 25-ton press used to make pressed pellets.

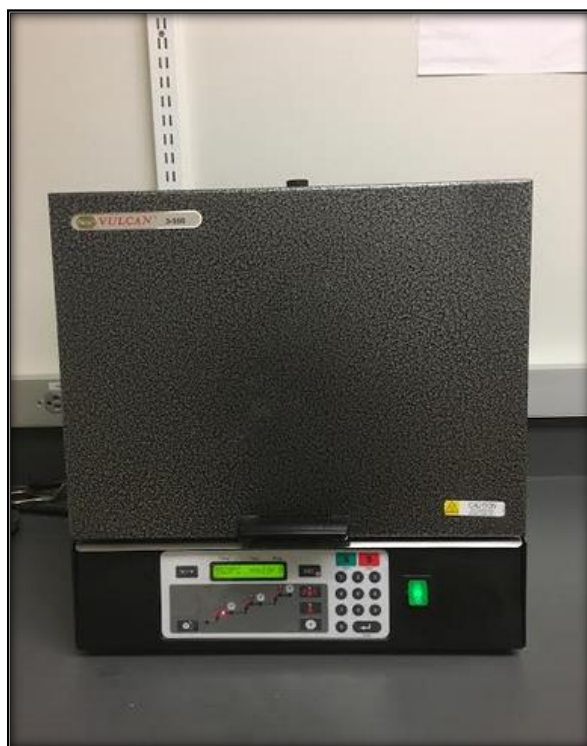


**Figure 12.** This photograph shows a muffle furnace where samples were melted at 1000 °C in graphite crucible.



**Figure 13.** This photograph shows pressed pellets and fusion beads undergoing geochemical analysis in the Rigaku ZSX-3 XRF machine.

## RESULTS

### Petrography

Samples from the five volcanoes show some similarities as well as differences in their mineralogy and textures. Samples were associated with the Kohala (KO), Hualalai (HU), Mauna Kea (MK), Mauna Loa (ML), and Kilauea (KI) volcanics. Mineralogy and textures were characterized using an Olympus Research-grade petrographic polarizing microscope with a digital camera. The majority of rocks studied were basalts, aphanitic to porphyritic in texture. These rocks had varying modal percentages of plagioclase, olivine, pyroxene, and opaques. Some samples displayed vesicular textures.

### *Kohala Volcanics*

The rock samples taken from the Kohala lava flows are all basalts. Samples from Kohala have a range in plagioclase and olivine phenocrysts from about  $< 0.1$  cm to 0.5 cm in size. The Kohala volcanic rocks are mainly fine-grained to porphyritic and vesicular in texture. Figure 15 shows the porphyritic texture, whereas the sample from figure 16 is aphanitic. The groundmass of the Kohala volcanics are composed of opaques, olivine, plagioclase and pyroxene minerals. Modal percentages for the rock were approximated. Based on this approximation, the rock sample from figure 15 is approximately 60 % plagioclase and 40 % opaques. (Figure 15) The rock sample from figure 16 is approximately 55 % plagioclase, 35 % olivine, 9 % opaques, and 1% pyroxene (Figure 16).

### ***Hualalai Volcanics***

The rock samples taken from the Hualalai lava flows are basaltic in composition. Samples from Hualalai have a range in phenocryst size from about 0.1 cm to 0.3 cm in size. The sample from figure 17 is porphyritic and vesicular in texture. The groundmass is composed of opaques, olivine, pyroxene, and plagioclase. Modal percentages for this rock were 50 % plagioclase, 30 % olivine, 15 % opaques, and 5 % pyroxene (Figure 17). The Hualalai volcanic samples are predominantly fine-grained, with phenocrysts and vesicular textures.

### ***Mauna Kea Volcanics***

The rock samples taken from the Mauna Kea lava flows are all basaltic. The sample from figure 18 is porphyritic, but not vesicular in texture, however, the sample from figure 19 is porphyritic and vesicular in nature. The groundmass is composed of opaques, olivine, pyroxene and plagioclase. Modal percentages for the sample in figure 18 are 50 % plagioclase, 35 % olivine, 15 % opaques, and 50 % plagioclase, 30 % opaques, 10 % olivine, and 10 % pyroxene for the sample shown in figure 19. Some Mauna Kea volcanic samples are coarser grained and contain phenocrysts ranging from about 0.2 cm to 0.6 cm in size (Figures 18, 19).

### ***Mauna Loa Volcanics***

The rock samples taken from the Mauna Loa lava flows are all basaltic. Samples from the Mauna Loa lava flows have a range in phenocryst size from about 0.1 cm to 0.2 cm in size. Figure 20 shows a porphyritic and vesicular basalt. The groundmass is composed of opaques, olivine, and plagioclase. Modal percentages are approximated as 45 % plagioclase, 30 % olivine, and 25 % opaques. Samples from the Mauna Loa lava flows are coarser grained and contain



large crystals, which are easily visible to the unaided eye. Some of these rock samples have crystals ranging from about 1 cm to 4 cm in size, predominantly olivine and pyroxene crystals are the simplest to see within the hand-sized rock samples.

### ***Kilauea Volcanics***

The rock samples taken from the Kilauea lava flows are all basaltic rocks. The rock samples from the Kilauea lava flows have phenocrysts which range from 0.2 cm to 0.4 cm. These samples also display vesicular and porphyritic textures. The groundmass is mainly composed of plagioclase and olivine. The modal percentages of the minerals in this rock are approximately 65 % plagioclase, 30 % olivine, 5 % opaques (Figure 21).

### **Comparisons**

All of the samples are similar in that they are all basaltic rocks, with at least 55 % plagioclase, 4 % opaques, and 5 % olivine within their approximation of their modal percentages. Most of the rock samples are vesicular in texture, with the exception of the Mauna Kea rocks from sample location MK-1 (Figure 6, 18). The rock samples are predominantly porphyritic in texture, with the exception of Kohala rocks from sample location KO-2 (Figure 6, 16). In contrast to the other rocks, the Kohala rocks from sample location 2 are aphanitic in texture. Lastly, the rocks range in crystal size from < 0.1 cm to 3 cm. However, the crystal sizes within the rock samples mainly range from approximately 0.1 cm to 0.3 cm. This range can be seen in figure 14.

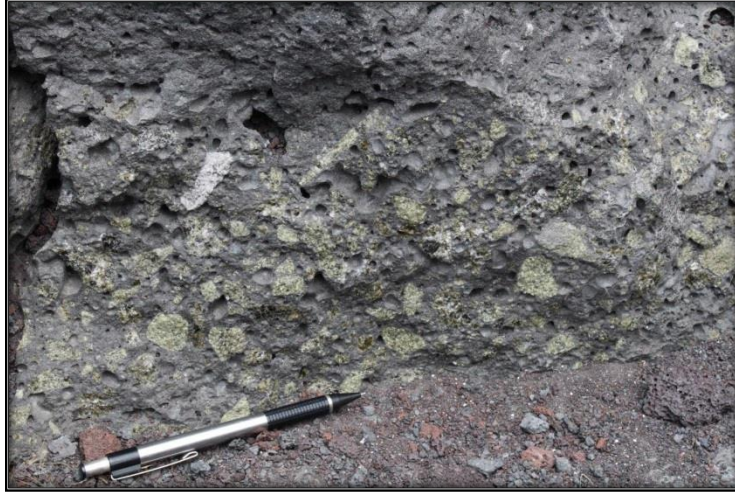


**Figure 14.** A rock sample, showing the variety in texture and crystal size (~ 3 cm) of peridotite xenoliths.

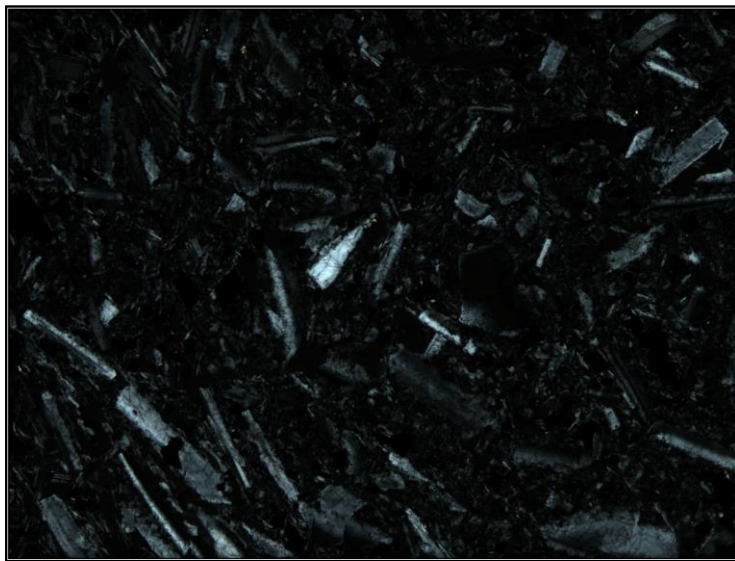


**Figure 15.** Photomicrograph of a basalt lava flow from Kohala (Location 1 from Figure 6, KO-1). Note the large plagioclase phenocrysts, opaques in the matrix, as well as small vesicles. The magnification used for this photomicrograph is 4.0 X and the photomicrograph is in cross-polarized light (XPL).

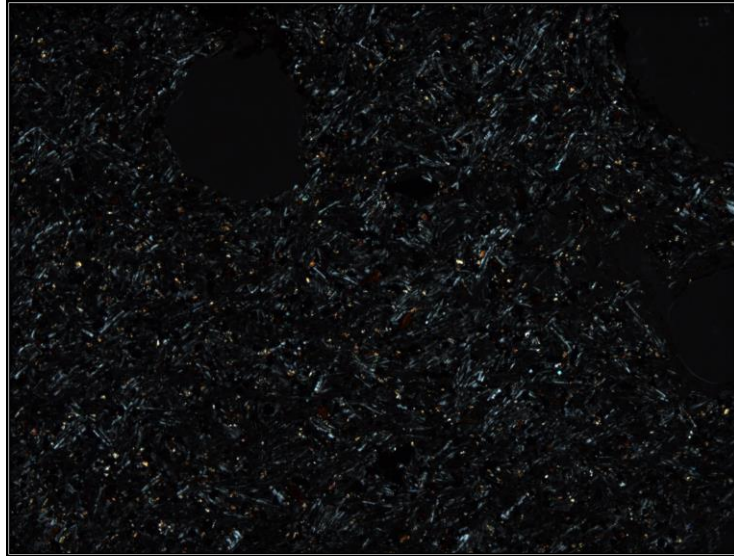


**Figure 16.** Photomicrograph of a basalt lava flow from Kohala (Location 2 from Figure 6, KO-2). Note the groundmass composed mainly of small olivine and plagioclase minerals in the matrix. In addition, note the vesicles shown in this photomicrograph. The magnification used for this photomicrograph is 4.0 X and the photomicrograph is in XPL.

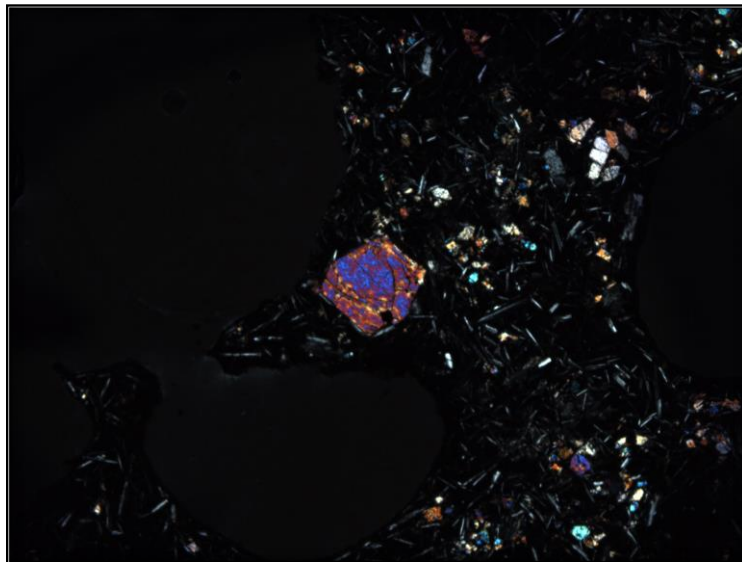


**Figure 17.** Photomicrograph of a basalt lava flow from Hualalai (Location 1 from Figure 6, HU-1). Note the large olivine phenocryst, as well as the matrix composed of smaller olivine, pyroxene and plagioclase minerals in the matrix. There are also dark colored round circles in this photomicrograph, which are vesicles. The magnification used for this photomicrograph is 4.0 X and the photomicrograph is in XPL.

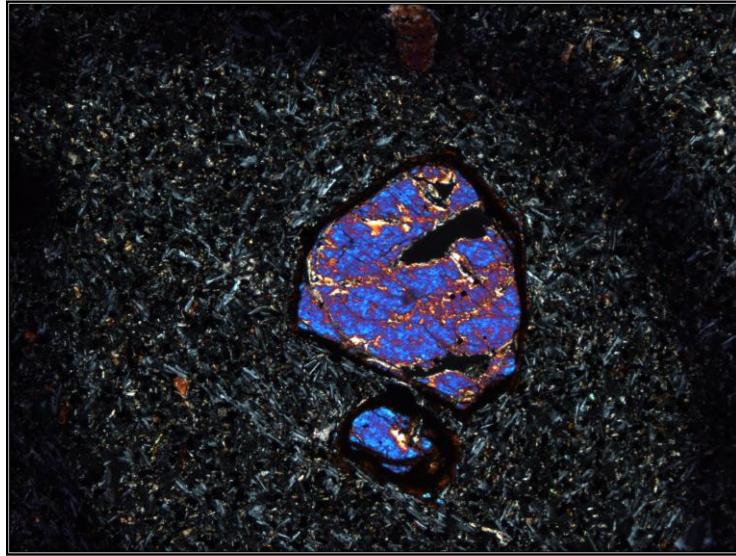


**Figure 18.** Photomicrograph of a basalt lava flow from Mauna Kea (Location 1 from Figure 6, MK-1). Note the two large olivine phenocrysts with oxide rings, as well as the matrix composed of predominantly plagioclase minerals. The magnification used for this photomicrograph is 4.0 X and the photomicrograph is in XPL.

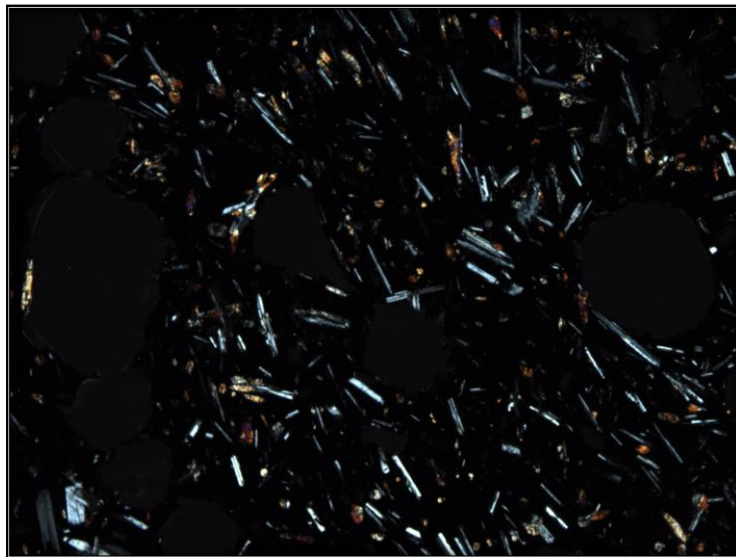


**Figure 19.** Photomicrograph of a basalt lava flow from Mauna Kea (Location 3 from Figure 3, MK-3). Note the vesicles, the plagioclase, olivine, and pyroxene crystals in the matrix. The magnification used for this photomicrograph is 4.0 X and the photomicrograph is in XPL.





**Figure 20.** Photomicrograph of a basalt lava flow from Mauna Loa (Location 4 from Figure 6, ML-4). Note the olivine phenocrysts as well as plagioclase in the matrix. This photomicrograph also contains vesicles. The magnification used for this photomicrograph is 4.0 X and the photomicrograph is in XPL.

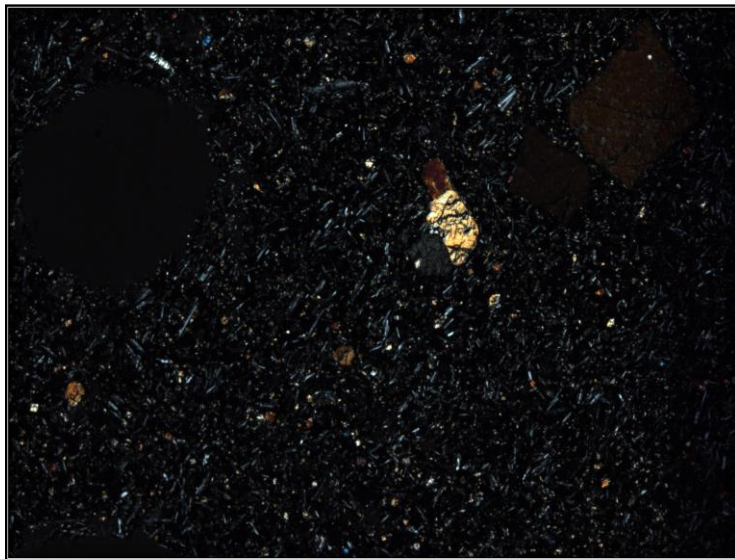


**Figure 21.** Photomicrograph of a basalt lava flow from Kilauea (Location 6 from Figure 6, KI-6). Note the large olivine phenocrysts with high relief, plagioclase, and its vesicular texture. The magnification used for this photomicrograph is 4.0 X and the photomicrograph is in XPL.

## **Geochemical Results**

### ***Kohala Volcanics***

The samples from the Kohala lava flows range in  $\text{SiO}_2$  contents from about 45% to 60%, while the  $\text{TiO}_2$  value ranges from about 0.99% to 3.4%. The CaO values range from approximately 2.9% to 7.9 % and MgO from about 1.2 % to 3.8 %.  $\text{Al}_2\text{O}_3$  values are relatively high and are in the range of 15% to 21 %.

### ***Hualalai Volcanics***

The samples from the Hualalai lava flows range in percentage of  $\text{SiO}_2$  from about 46% to 51.5%, while the  $\text{TiO}_2$  value ranges from approximately 1.6 % to 2.5 %. The CaO content, ranges from approximately 8.1 % to 11 %, while the MgO component ranges from about 6 % to 13.9 %. The ranges of  $\text{Al}_2\text{O}_3$  are approximately 13.9 % to 16.5 %.

### ***Mauna Kea Volcanics***

The rock samples from the Mauna Kea lava flows range in percentage of MgO from about 3.2 % to 6 %, while the  $\text{Al}_2\text{O}_3$  value ranges from approximately 13.8 % to 16 %. The percentage of  $\text{SiO}_2$  ranges from about 46 % to 50.5 %, while the CaO component ranges from approximately 6.1 % to 11.9 %. Lastly, the ranges of the percentages of  $\text{TiO}_2$  approximately 2.4 % to 4.5 %.

### ***Mauna Loa Volcanics***

The samples from the Mauna Loa lava flows range in percentage of  $\text{SiO}_2$  from about 47.5 % to 51.5 %, while the  $\text{TiO}_2$  value ranges from about 2.1 % to 2.5 %. The CaO value ranges

from approximately 10.5% to 11.5 %, and the MgO value ranges from about 5.9 % to 8.1 %. The samples range in percentage of  $\text{Al}_2\text{O}_3$  value ranges from approximately 12 % to 14.6 %.

### ***Kilauea Volcanics***

The rock samples from the Kilauea lava flows range in percentage of MgO from about 6 % to 12 %, while the  $\text{Al}_2\text{O}_3$  value ranges from approximately 10.1 % to 13.9 %. The rock samples from the Kilauea lava flows range in percentage of  $\text{SiO}_2$  from about 46.5 % to 49.5 %. The  $\text{TiO}_2$  value ranges from about 2.4 % to 2.9 %. The CaO value ranges from about 9.9 % to 10.9 %.

### **Distinction of Geochemistry across the Five Volcanoes**

There is a different geochemical signature among the five volcanoes. All the Kohala volcanics plot within the alkalic part of the graph (Figure 47). The Hualalai volcanics mainly plot in the tholeiitic part of the graph, while the Mauna Kea volcanics mainly plot in the alkalis part of the graph. Lastly, the Mauna Loa volcanics mainly plot in the tholeiitic part of the chart, as well as the Kilauea volcanics. Within the tectonic discrimination diagrams the rock samples from all of the volcanoes mainly plot in the following regions: A in Figure 48 “within plate basalts”, OIT in figure 49 ocean island tholeiite, OIA in figure 49 ocean island alkali basalt. Those regions imply the origins of the rock sample (Figure 48, 49). This depiction of difference in geochemical signature, relates to the overall stage of development for each volcano.

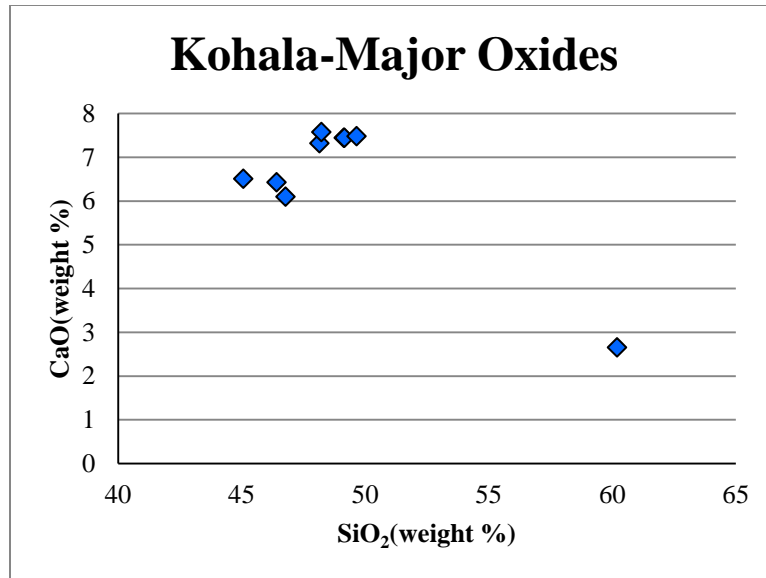


**Figure 22.** CaO vs. SiO<sub>2</sub> graph from Kohala volcanics.

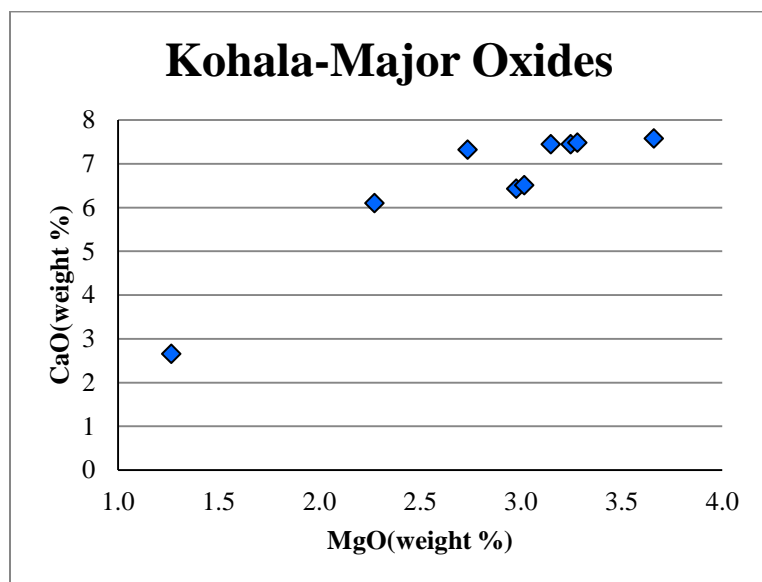


**Figure 23.** CaO vs. MgO graph from Kohala volcanics.



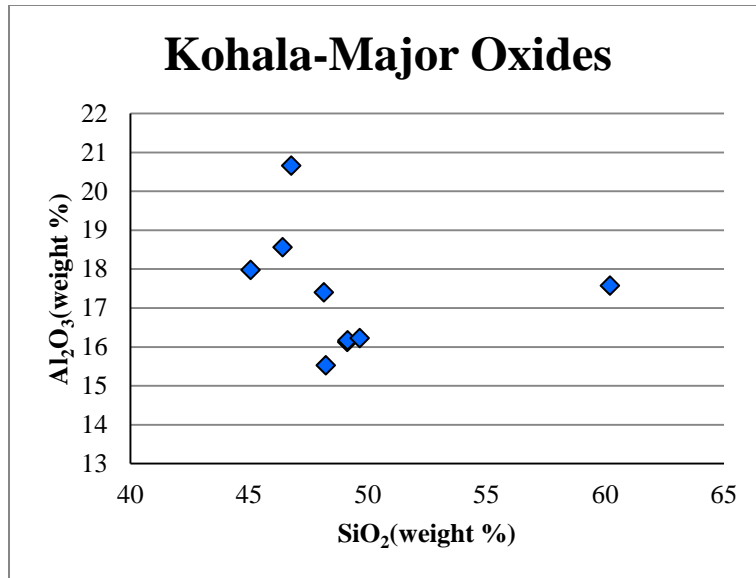


**Figure 24.** Al<sub>2</sub>O<sub>3</sub> vs. SiO<sub>2</sub> graph from Kohala volcanics.

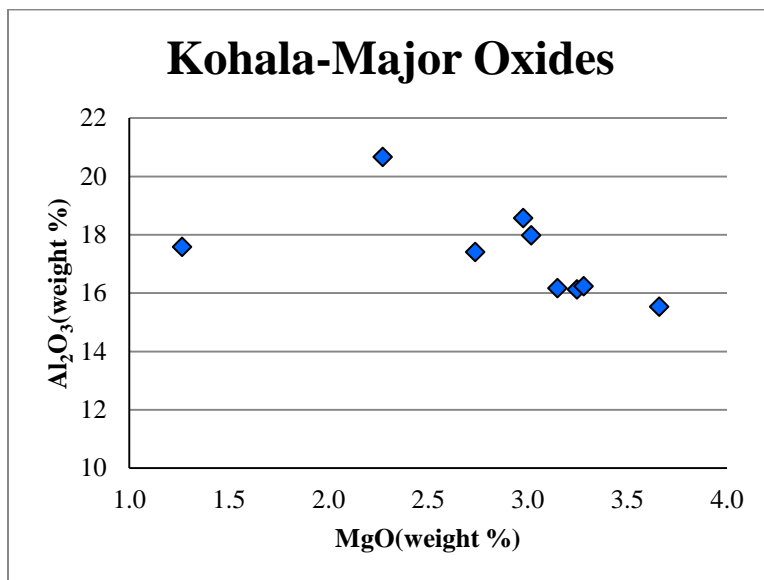


**Figure 25.** Al<sub>2</sub>O<sub>3</sub> vs. MgO graph from Kohala volcanics.

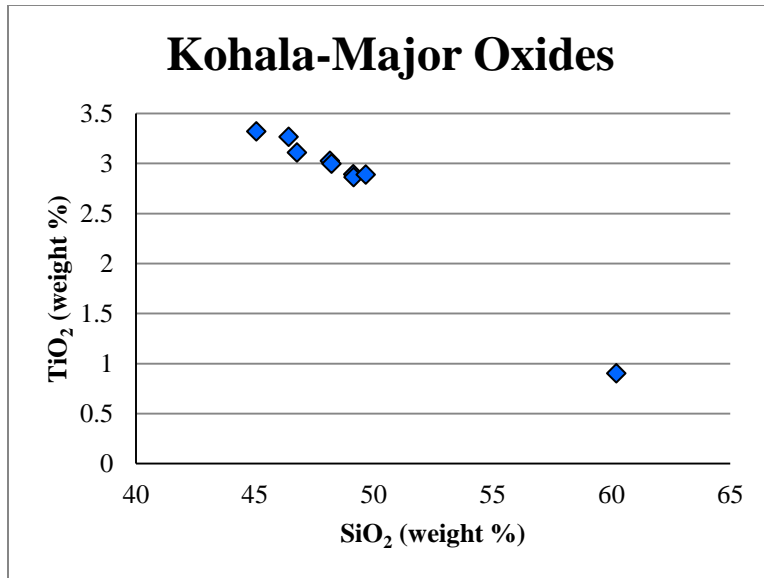


**Figure 26.** TiO<sub>2</sub> vs. SiO<sub>2</sub> graph from Kohala volcanics.

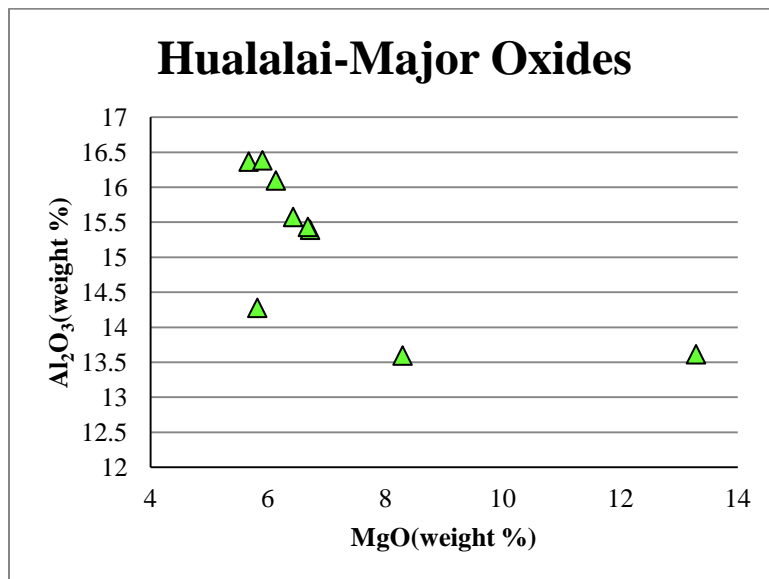


**Figure 27.** Al<sub>2</sub>O<sub>3</sub> vs. MgO graph from Hualalai volcanics.

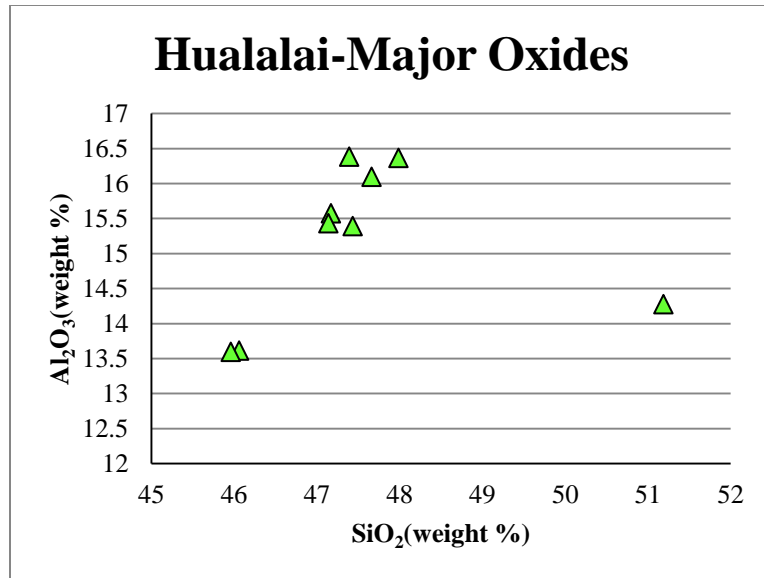


**Figure 28.**  $\text{Al}_2\text{O}_3$  vs.  $\text{SiO}_2$  graph from Hualalai volcanics.

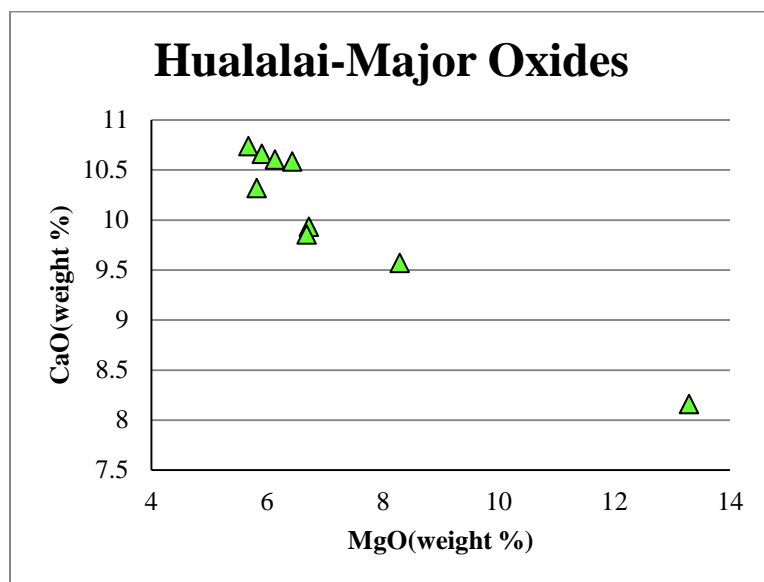


**Figure 29.**  $\text{CaO}$  vs.  $\text{MgO}$  graph from Hualalai volcanics.

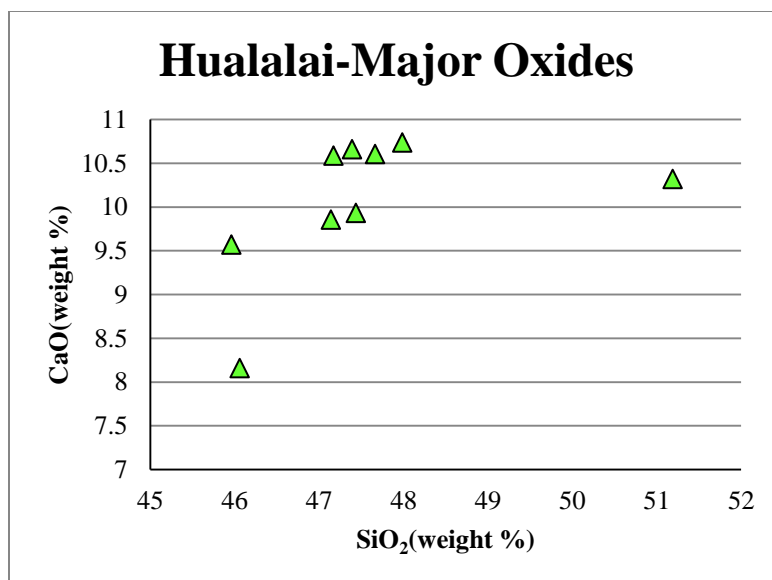


**Figure 30.** CaO vs. SiO<sub>2</sub> graph from Hualalai volcanics.

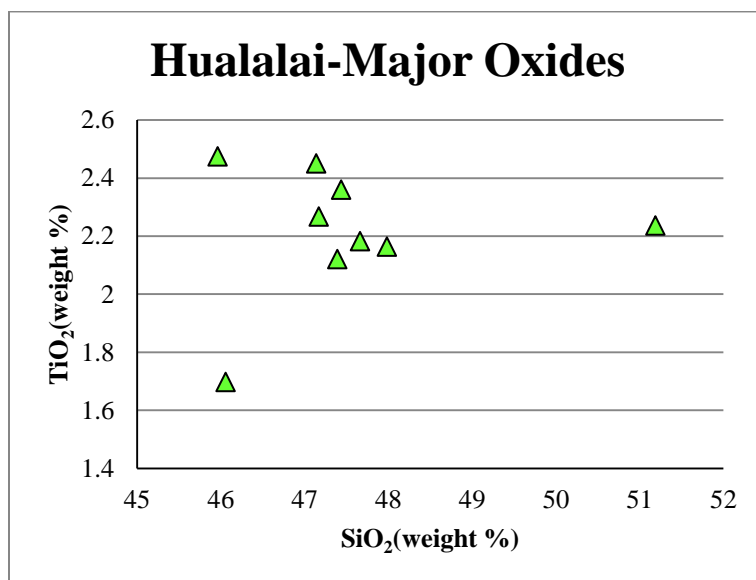


**Figure 31.** TiO<sub>2</sub> vs. SiO<sub>2</sub> graph from Hualalai volcanics.

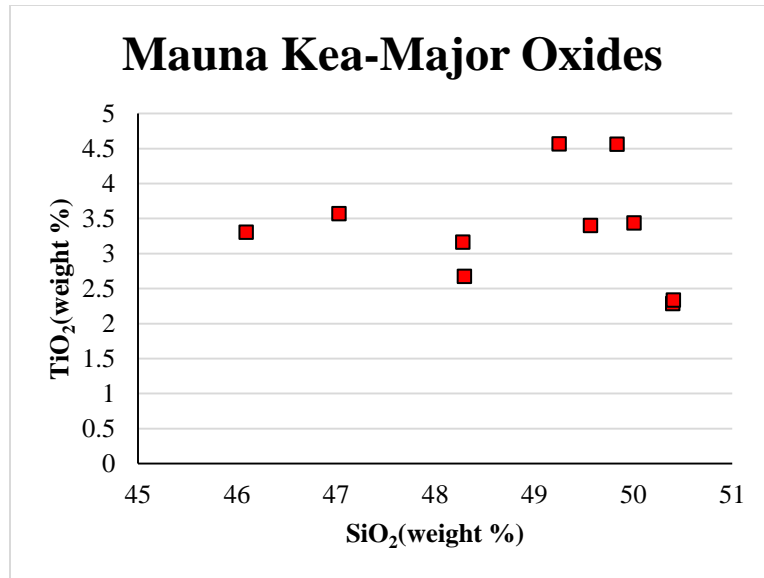


**Figure 32.** TiO<sub>2</sub> vs. SiO<sub>2</sub> graph from Mauna Kea volcanics.

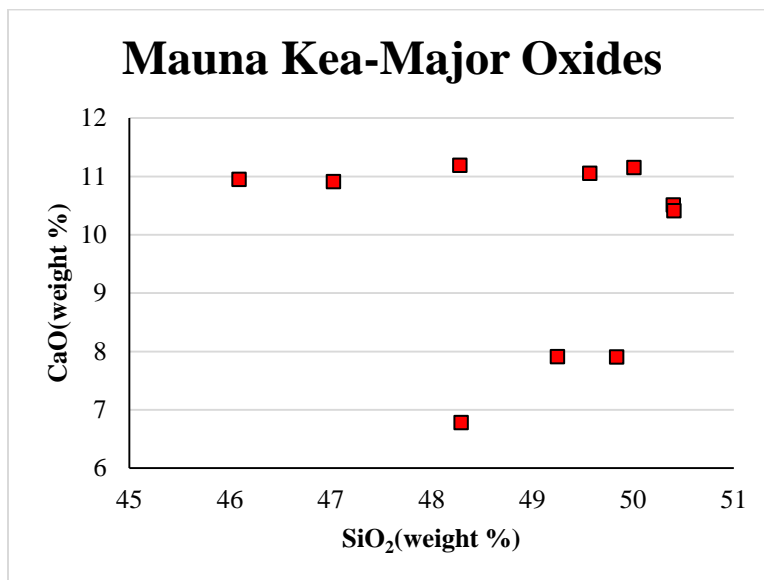


**Figure 33.** CaO vs. SiO<sub>2</sub> graph from Mauna Kea volcanics.

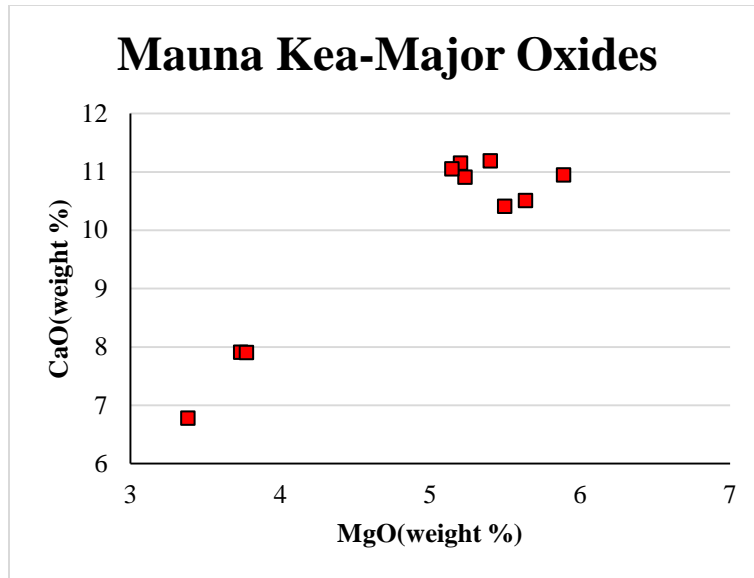


**Figure 34.** CaO vs. MgO graph from Mauna Kea volcanics.

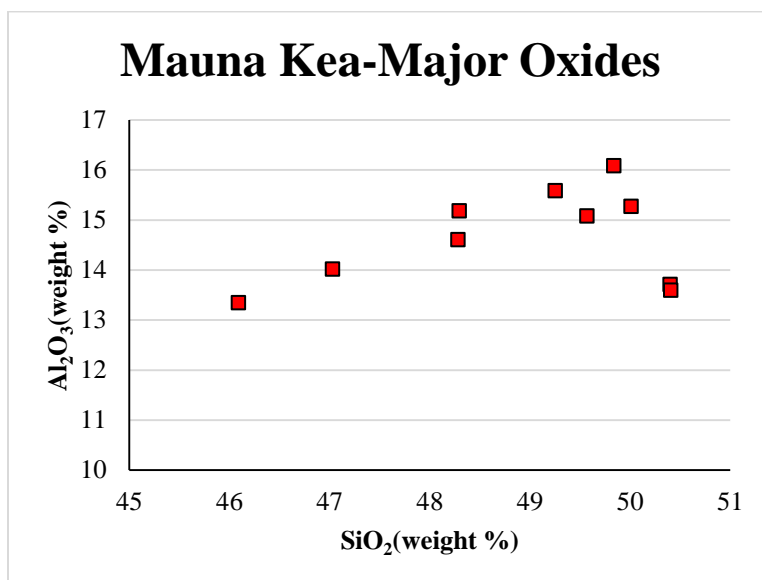


**Figure 35.** Al<sub>2</sub>O<sub>3</sub> vs. SiO<sub>2</sub> graph from Mauna Kea volcanics.

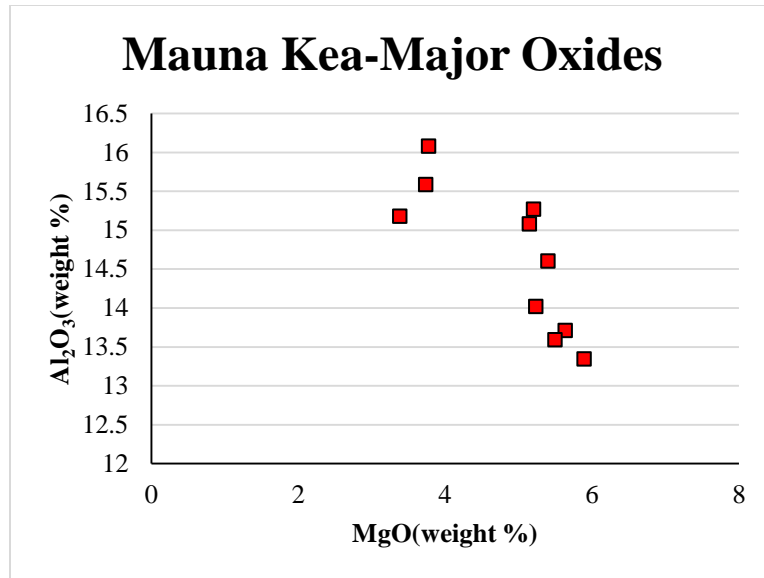


**Figure 36.** Al<sub>2</sub>O<sub>3</sub> vs. MgO graph from Mauna Kea volcanics.

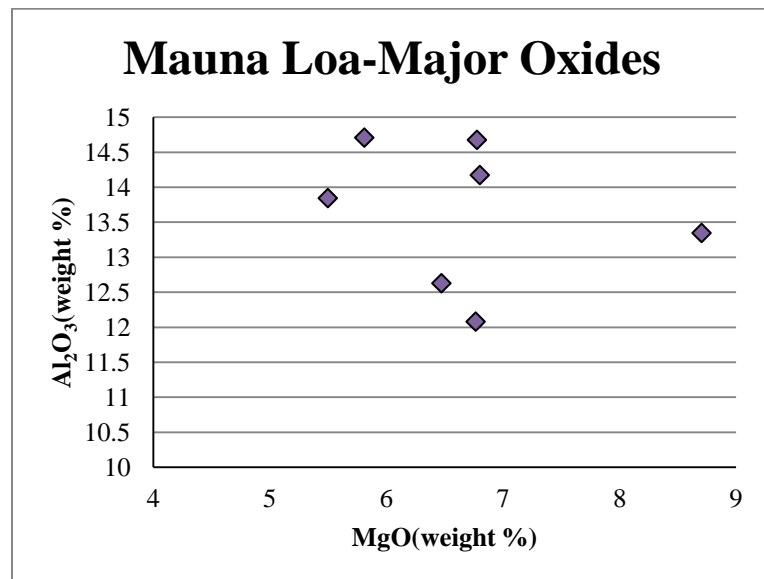


**Figure 37.** Al<sub>2</sub>O<sub>3</sub> vs. MgO graph from Mauna Loa volcanics.

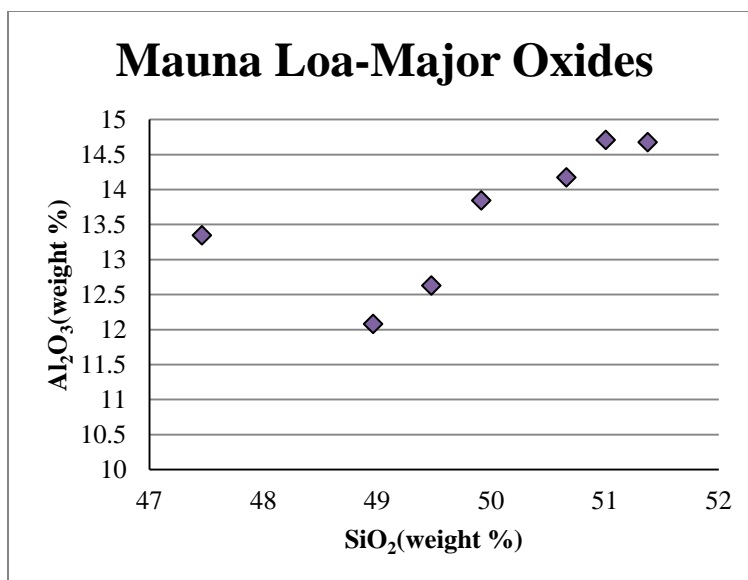


**Figure 38.**  $\text{Al}_2\text{O}_3$  vs.  $\text{SiO}_2$  graph from Mauna Loa volcanics.

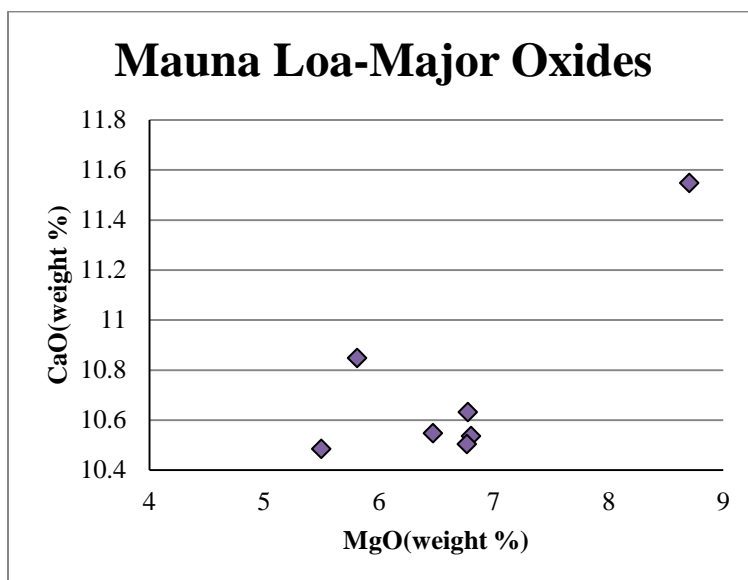


**Figure 39.**  $\text{CaO}$  vs.  $\text{MgO}$  graph from Mauna Loa volcanics.



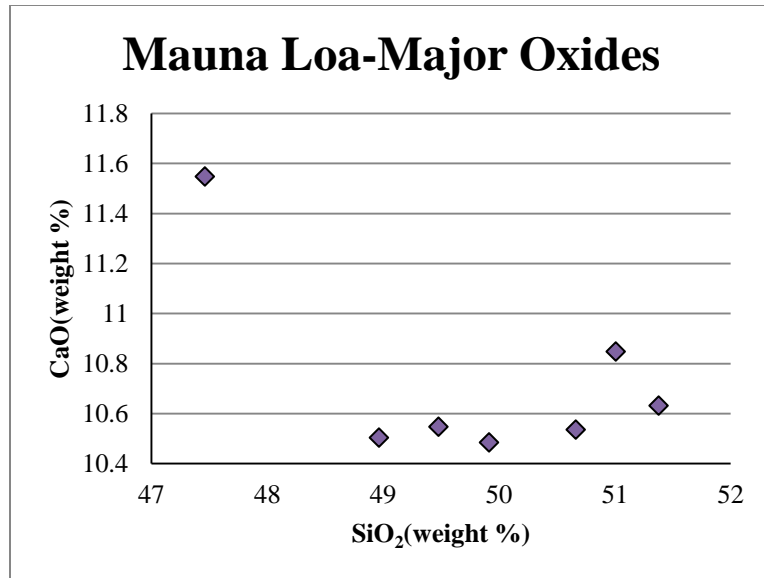


**Figure 40.** CaO vs. SiO<sub>2</sub> graph from Mauna Loa volcanics.

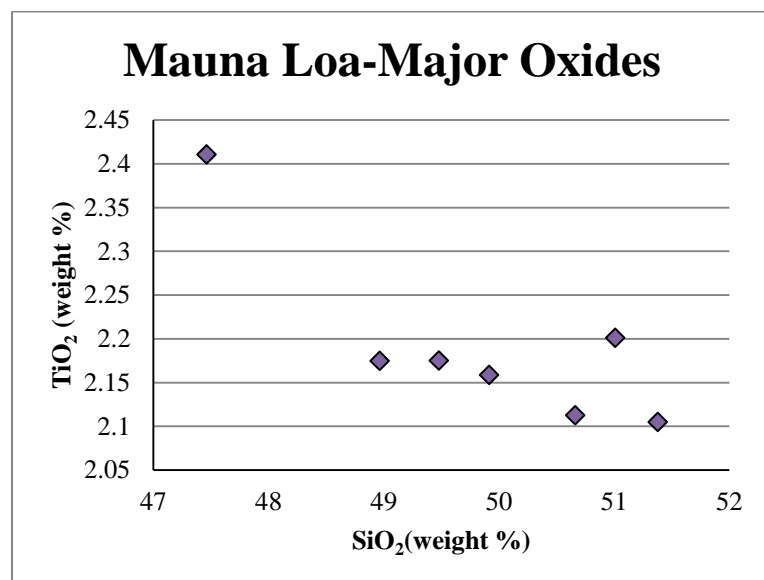


**Figure 41.** TiO<sub>2</sub> vs. SiO<sub>2</sub> graph from Mauna Loa volcanics.

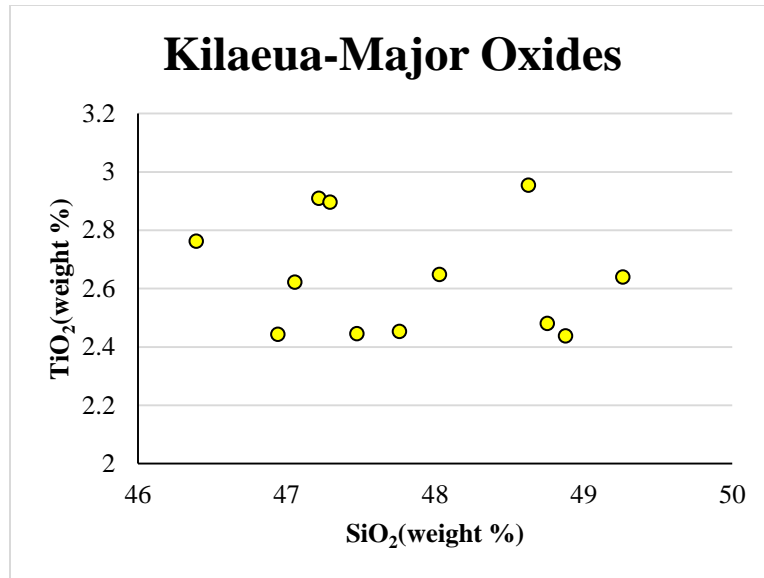


**Figure 42.** TiO<sub>2</sub> vs. SiO<sub>2</sub> graph from Kilauea volcanics.

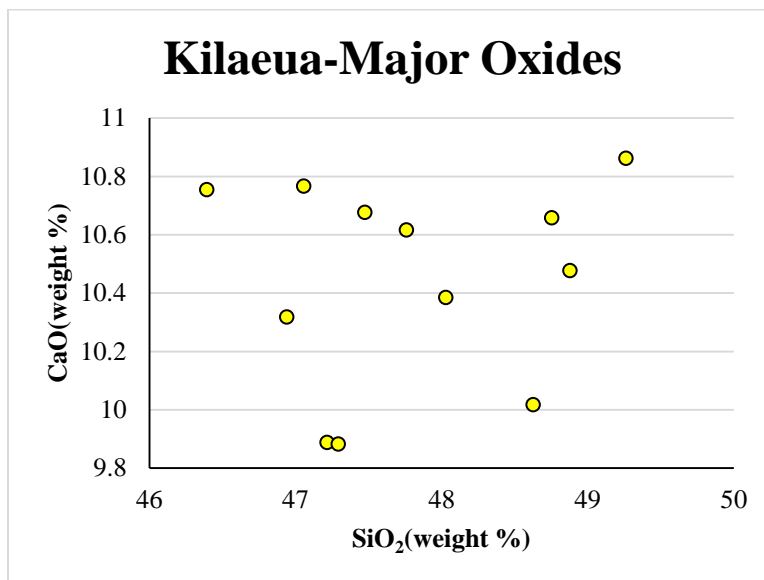


**Figure 43.** CaO vs. SiO<sub>2</sub> graph from Kilauea volcanics.

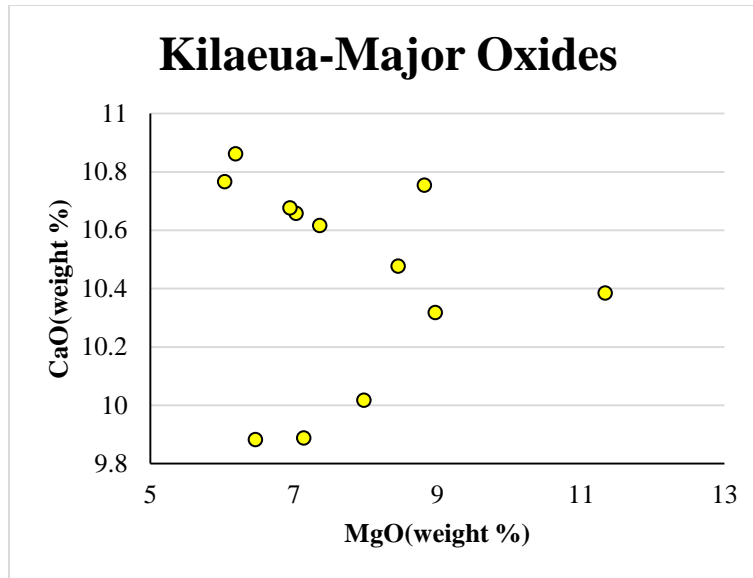


**Figure 44.** CaO vs. MgO graph from Kilauea volcanics.

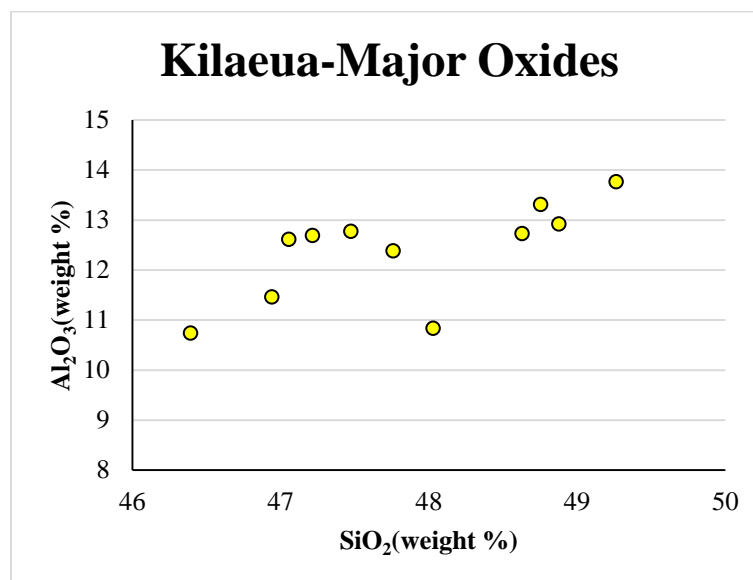


**Figure 45.** Al<sub>2</sub>O<sub>3</sub> vs. SiO<sub>2</sub> graph from Kilauea volcanics.

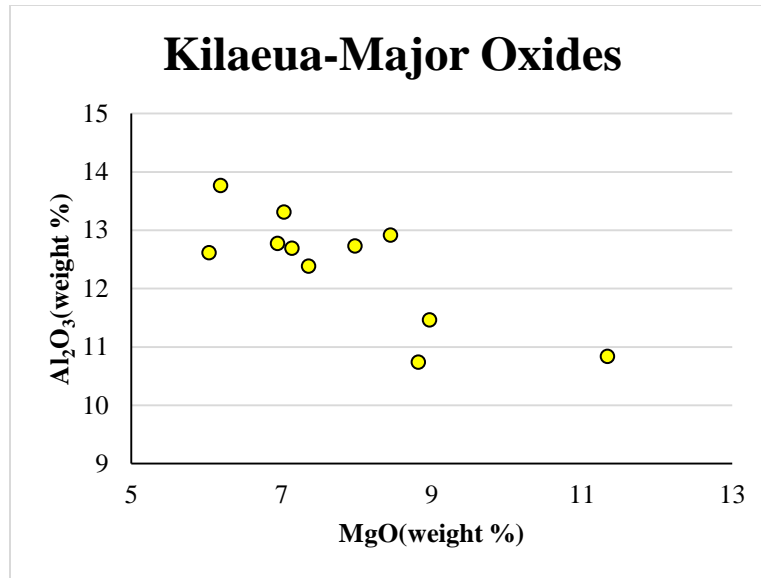


**Figure 46.** Al<sub>2</sub>O<sub>3</sub> vs. MgO graph from Kilauea volcanics.

## DISCUSSION/CONCLUSION

The Hawaiian island is located on the Pacific plate, and therefore, it is expected that the samples would plot in the “A” region (within plate basalts) of the discrimination diagram that identifies the tectonic setting in which these rocks formed (Figure 48). Figure 49 shows the samples plotting as ocean island basalts. These samples are separated by their geochemical composition, where “OIT” represents ocean island tholeiitic basalts and “OIA” represents ocean island alkali basalts (Figure 49). There is one sample that plots in the “MORB” or mid-ocean ridge basalt. This sample is likely an outlier, as it is poorly representative of the samples taken from the island as a whole. The points that plot outside of the quadrilateral shape labeled “A” poorly represent the sample and are outliers as well. The two points that are outside of the shape from figure 50, is also poorly representative of the samples as a whole. However, it is important to note that Kohala does not mainly fall into the “D” or “within plate basalts” region of the diagram (Figure 50). Instead, it falls into the region of the diagram that is labeled “C”, which

represents “continental arc basalts”. This may be due to its chemical compositional change.

Compared to the other volcanoes, Kohala is the oldest. Its flows are the oldest as well, as it is now extinct. This could be the reason for it falling into this section of the diagram.

Ocean island basalts are characterized by the composition of the source, degree of partial melting and composition of residual phases, and subsequent fractional crystallization (Frost, 2014). Alkali and tholeiitic basalts are different in chemical composition, because the source of the mantle magma differs in various ways (Frost, 2014). As stated in the geologic setting of this thesis, the geochemistry of these lavas could be changing for different reasons.

One reason for variation in chemical composition could be due to the reaction of the oceanic crust with the seawater (Harmon & Parker, 2011). Also, “intrusion and extrusion of intraplate magmas also change the composition of the oceanic crust after its generation at the mid-ocean ridge” (Harmon & Parker, 2011). It is also possible that this chemical composition change is due to partial melting and crystallization (Frost 2014; Harmon & Parker 2011). With partial melting and fractional crystallization, different minerals will form crystals at different times. This will affect its density. Denser minerals will settle to the bottom, which will affect the chemical composition of the outpourings of the magma. The volcano will extrude lavas and will not contain much of the minerals because they have settled.

Therefore, ocean island basalts can differ in chemical composition due to the source of the magma being different. For example, the degree of the mantle magma melting is different, as well as the depth of the mantle from which the source is taken (Frost, 2014). In other words, they differ in their origins. Alkali basalts are characterized by smaller degrees of partial melting at greater depths, whereas tholeiitic basalts are characterized by larger degrees of partial melting at shallow depths (Frost, 2014). This differential melting causes a change in the chemistry of the

outpourings of the lava. Depending on the minerals that crystallize out of the magma, this indicates the incompatibility the crystals have with the melt.

The reason for these variations in chemical composition may also be “due to the degrees and depths of partial melting and chemical heterogeneities in the upper mantle (Harmon & Parker, 2011). Usually, the incompatible elements are higher in concentration where there are chemical heterogeneities and are a reflection of the mantle plumes “causing age-progressive volcanic chains” (Harmon & Parker, 2011). This idea is similar to the age trend of the Hawaiian volcanoes, which change in chemical composition due to its location in relation to the mantle plume.

Among the five different volcanoes on the Hawaiian island, the main shield building stage has the highest degree of partial melting, whereas the pre- and post-shield stage lavas are produced at “relatively low degrees of melting” (Clague & Dalrymple 1987).

The chemical composition is a possible indication of the stage of development for a particular volcano. As shown in figure 47, there is a distinction between alkalic basalts and tholeiitic basalts. The alkalic portion of the graph indicates that the volcano is in the post shield stage (Figure 47). Alternatively, the tholeiitic section of the graph represents the volcano in the main shield stage. If the rock samples are plotting in more than one section of the graph, it is likely transitioning between stages. However, the data points do cluster in certain areas.

The pre-shield and post-shield stage is characterized by alkalic lavas, while the main building shield stage is characterized by tholeiitic lavas. The post-erosional or rejuvenation stage is characterized by alkali lavas (Clague & Dalrymple 1987).

Applying this idea to the data set, the Kohala volcanics fall in the alkalic portion of the diagram, indicating that it is in the post-shield stage. Because Kohala is alkalic and is therefore in

the post-shield stage, it will be entering the erosional stage of development. Kilauea mainly plots in the tholeiitic section of the graph, with the exception of one point, therefore it is likely in the main shield building stage of development. Hualalai, Mauna Kea, and Mauna Loa are transitioning from the main shield building stage to the post-shield stage indicated by their chemical compositions. There seems to be a north-westerly trend from Kilauea being in the main shield building stage to Kohala being in the post-shield stage. This is in the same direction of the Pacific plate motion.

These basaltic rock samples are all the source of a hotspot within the Hawaiian island. Therefore, the rock sample data points should plot within plate basalts and ocean island alkali/tholeiitic basalts. The geochemical discrimination diagrams are consistent with the geologic setting of the volcanoes, with Hualalai and Kohala representing oceanic island alkali basalts (OIA) and Mauna Loa and Kilauea plotting within the oceanic island tholeiitic field (Figure 48, 49). Ultimately, the data suggests that the chemical composition of the outpourings of lavas for these volcanoes are changing over time.

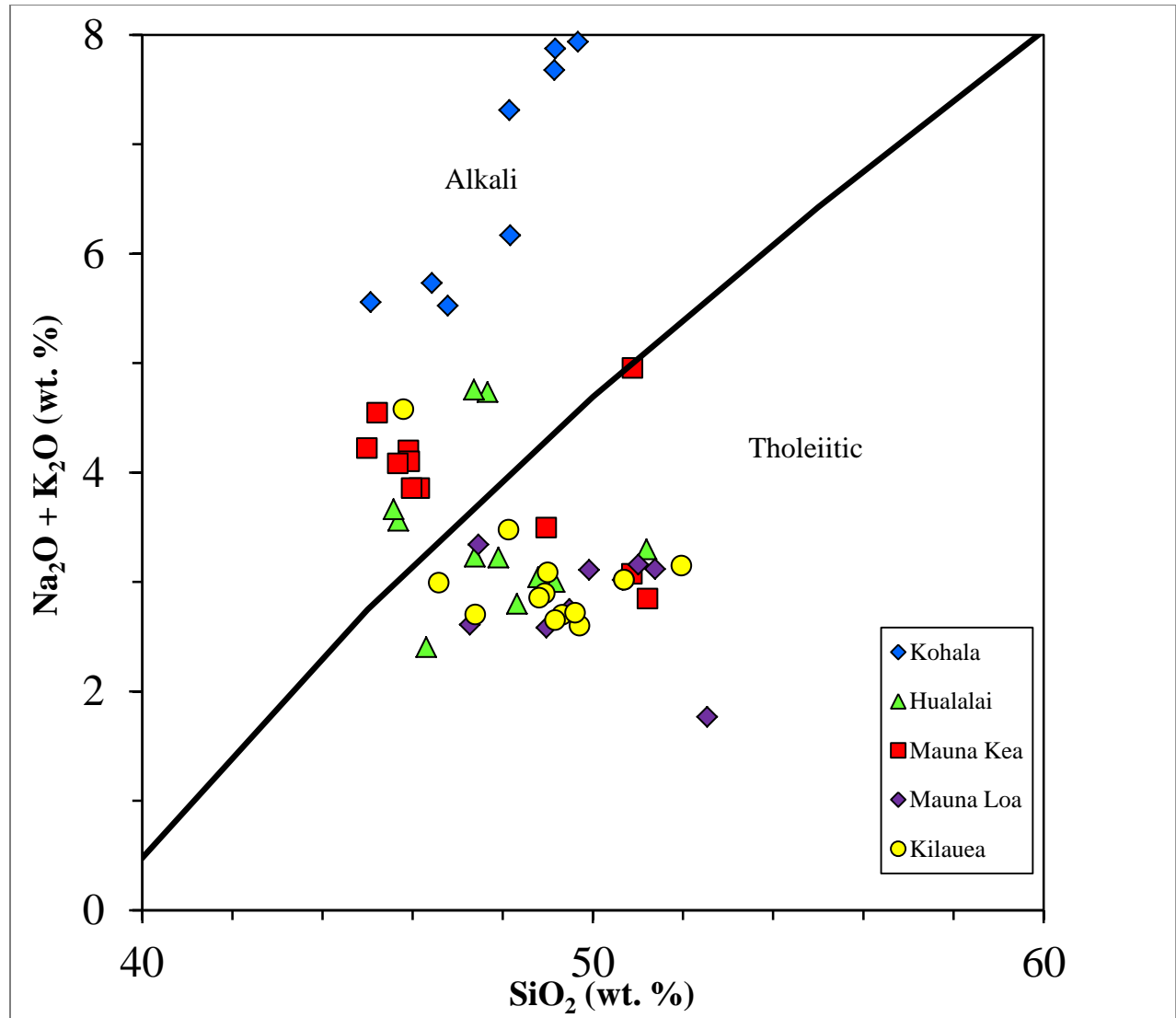


**Figure 47.** Total alkali vs. SiO<sub>2</sub> graph depicting tholeiitic and alkalic fields based on their chemical composition.



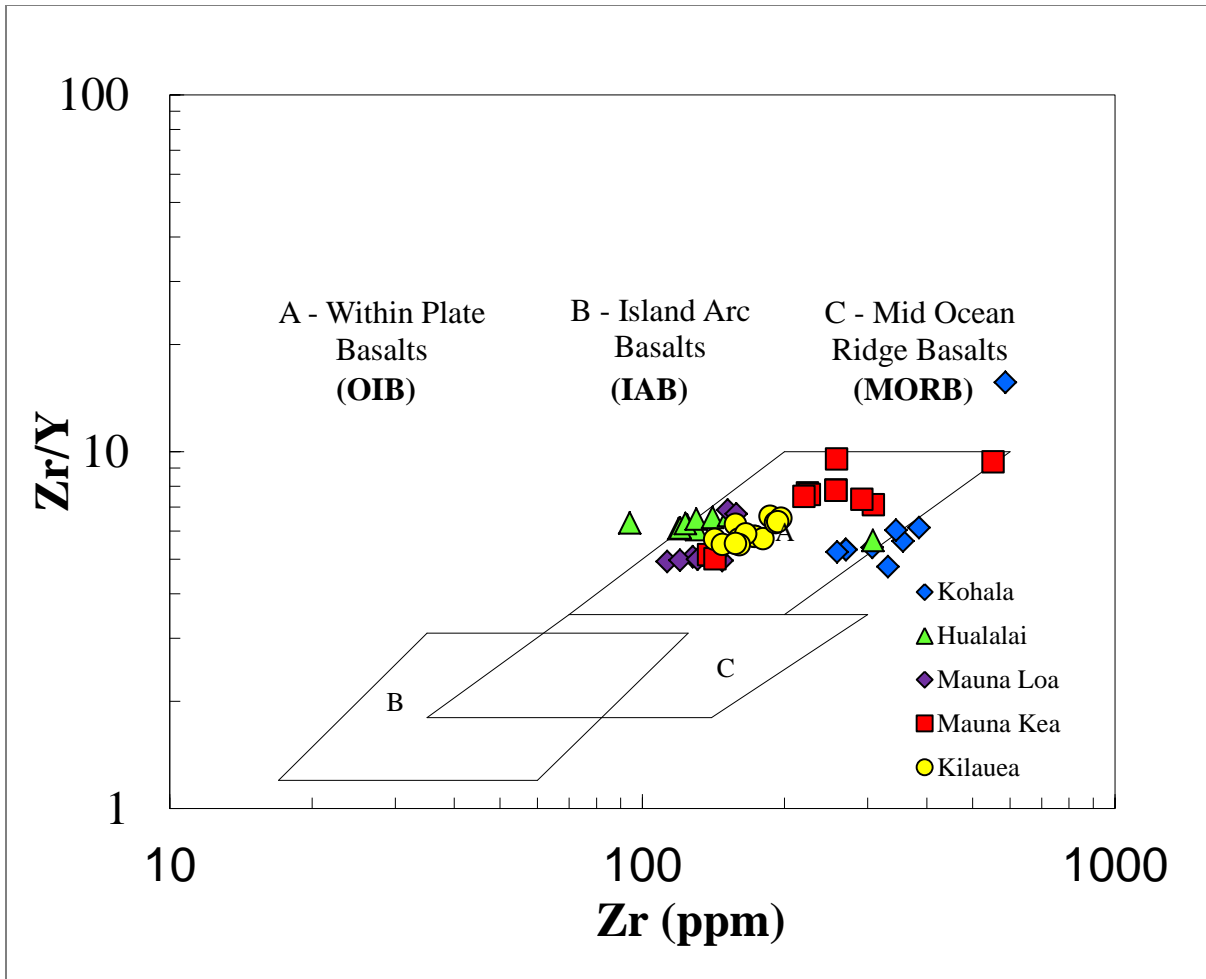


**Figure 48.** Tectonic discrimination diagram of Zr/Y vs. Zr showing the tectonic settings for basalt. Within-plate (OIB) basalts are related to mantle plume activity. Island arc (IAB) are formed in subduction zones. Mid-ocean ridge basalts (MORB are formed at oceanic spreading centers).

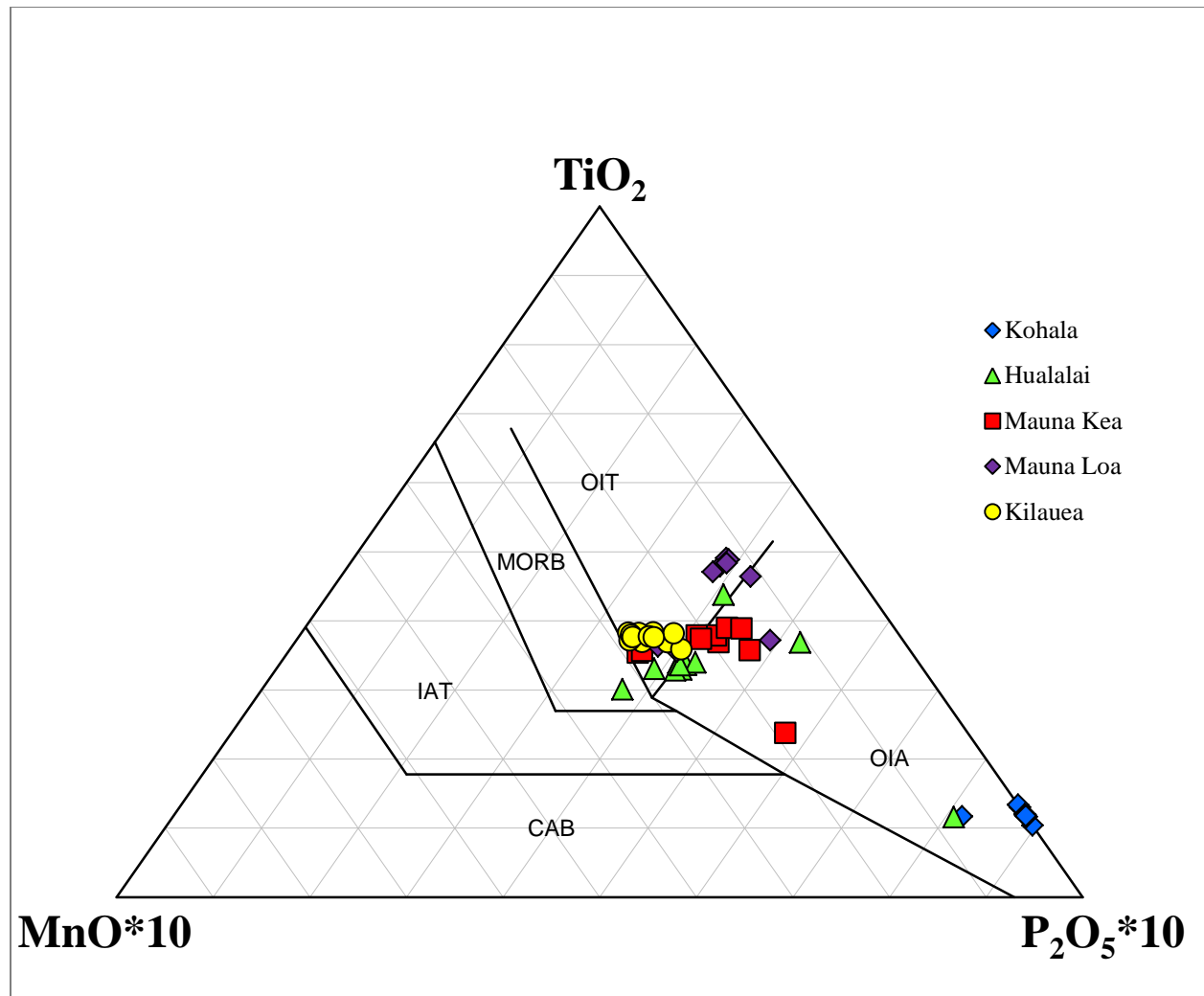


**Figure 49.** Tectonic discrimination diagram further defining tectonic settings of basalt generation. The Hawaii samples mainly fall in either the OIT (ocean island tholeiite) or the OIA (oceanic island alkali basalts).

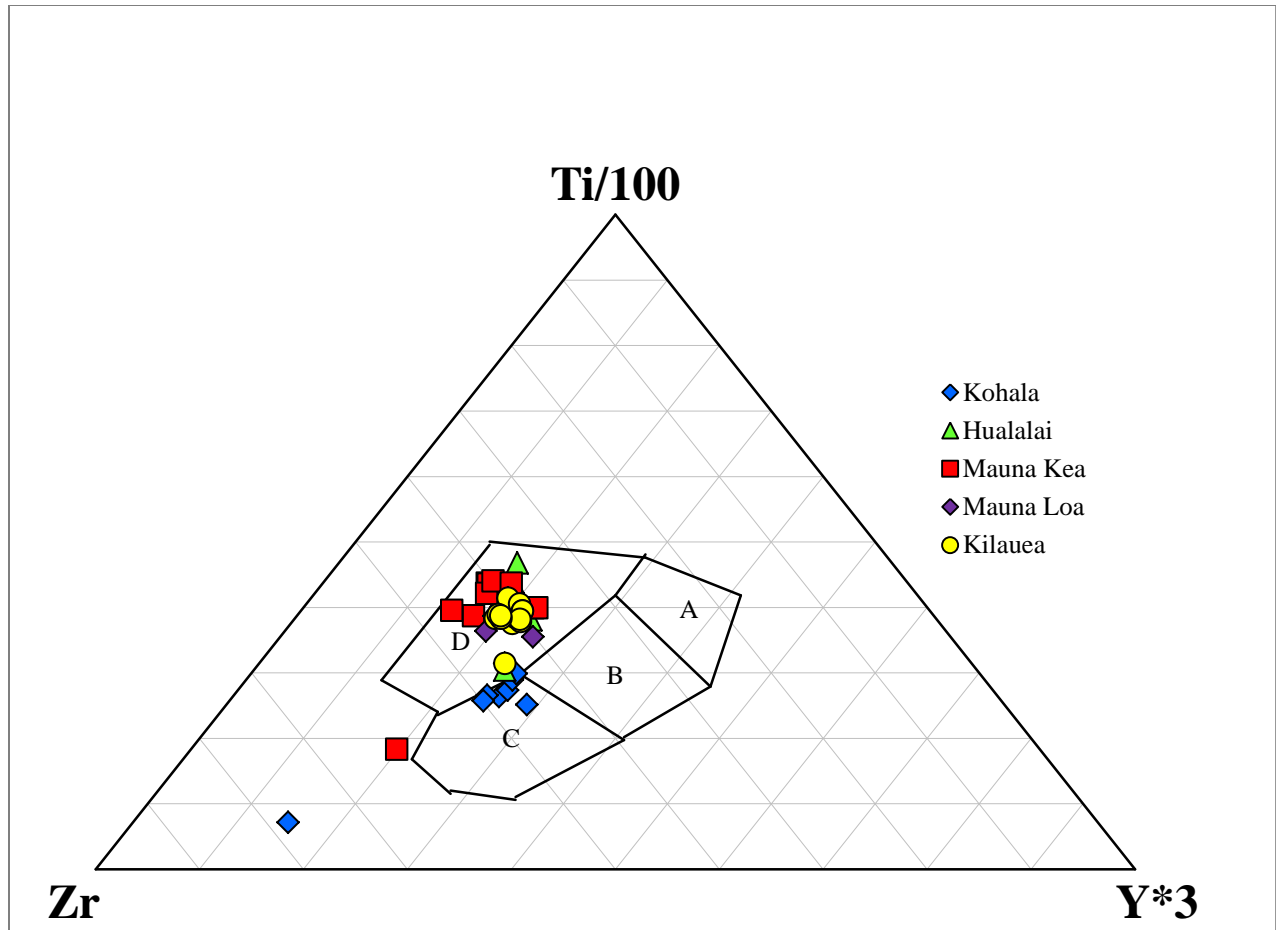


**Figure 50.** Tectonic discrimination diagram further defining tectonic settings of basalt generation. The Hawaii samples predominantly fall in either the “D” (Within Plate Basalts) or “C” (Continental Arc Basalt) portion of the graph.

## REFERENCES CITED

Clague, D. A., & Denlinger, R.P., 1994. Role of olivine cumulates in destabilizing the flanks of Hawaiian volcanoes. *Bulletin of Volcanology*, v. 56, p. 425-434.

Clague, D. A., 1987. Hawaiian xenolith populations, magma supply rates, and development of magma chambers. *Bulletin of Volcanology*, v. 49, p. 577-587.

Clague D. A., & Dalrymple G. B., 1987. The Hawaiian-Emperor volcanic chain. U.S. Geol. Survey Prof. Pap. 1350: pp. 5-54.

Chen, C., & Frey, F. A., 1985. Trace element and isotopic geochemistry of lavas from Haleakala volcano, East Maui, Hawaii: Implications for the origin of Hawaiian Basalts. *Journal of Geophysical Research*, v. 90, p. 8743-8768.

Frost, B. R. Frost, C. D., 2014. *Essentials of Igneous and Metamorphic Petrology*. New York, NY: Cambridge University Press.

Garcia, M., 2011. School of Ocean and Earth Science and Technology. Hawaiian Submarine Volcanism. <http://www.soest.hawaii.edu/microprobe/garcia-newspaper.html>;  
<https://www.soest.hawaii.edu/GG/HCV/credits.html>

Hanks, B., 2015. Hotspots: Mantle thermal plumes in Kious, J. & Tilling R., eds., *The Dynamic Earth: The story of plate tectonics*, United States Geological Survey,  
<http://pubs.usgs.gov/gip/dynamic/dynamic.html>

Harmon, R. S., Parker, A., 2011. *Frontiers in Geochemistry: Contribution of Geochemistry to the Study of the Earth*. West Sussex, UK: John Wiley & Sons, Ltd.

Jerram, D., Petford, N., 2011. *The Field Description of Igneous Rocks*, 2nd edition. West Sussex, UK: John Wiley & Sons, Ltd.

Strickler, M., 1997. Bowen's Reaction Series. University of Oregon.  
<http://jersey.uoregon.edu/~mstrick/AskGeoMan/geoQuerry32.html>

Tardona, M., 2011. Hawaiian Submarine Volcanism. School of Ocean and Earth Science and Technology. <https://www.soest.hawaii.edu/krubin/GG711/gg711-lect11-mary.pdf>

Tatsumi, Y., Goto, A., 1994. Quantitative Analysis of Rock Samples by an X-ray Fluorescence Spectrometer (I). *Rigaku Journal*. v. 11, No. 1, p. 40-59.

Thornberry-Ehrlich, T. L., 2017. *Geology of the Hawaiian Islands: Hawaii and Keating*. Colorado State University.  
[https://www.nature.nps.gov/geology/education/education\\_graphics.cfm](https://www.nature.nps.gov/geology/education/education_graphics.cfm)

United States Geological Survey, 2008, Jaggar Museum Display.

Watanabe, M., 2015. Sample Preparation for X-ray Fluorescence Analysis IV. Fusion bead method-part 1 basic principles. Rigaku Journal, v. 31, No. 2, p. 12-17.

Watson, J., 2011. U.S. Geol. Surv., General Interest Publications of the U.S. Geological Survey.  
*<https://pubs.usgs.gov/gip/volc/types.html>*

Yamada, Y., 2010. X-ray Fluorescence Analysis by Fusion Bead Method for Ores and Rocks. Rigaku Journal. v. 26, No. 2, p. 15-23.